

000
001
 **VIDEO****MIND**: A CHAIN-OF-LORA AGENT FOR
002 TEMPORAL-GROUNDED VIDEO REASONING
003

004 **Anonymous authors**
005 Paper under double-blind review
006

007 **ABSTRACT**
008

009 Videos, with their unique temporal dimension, demand precise grounded under-
010 standing, where answers are directly linked to visual, interpretable evidence. De-
011 spite significant breakthroughs in text-based reasoning with large language mod-
012 els, multi-modal reasoning – especially for videos – remains limited. In this work,
013 we fill this gap by introducing **VideoMind**, a novel video-language agent for
014 temporal-grounded video reasoning. Our method involves two key innovations:
015 (1) We identify four essential capabilities for grounded video reasoning and pro-
016 pose a role-based agentic workflow, comprising a **planner** to coordinate roles,
017 a **grounder** for temporal event localization, a **verifier** to assess event can-
018 didates, and an **answerer** for question answering. (2) To efficiently integrate
019 these roles during inference, we propose a novel **Chain-of-LoRA** mechanism,
020 where a unified base model with multiple LoRA adapters is leveraged to enable
021 seamless role switching, balancing efficiency and flexibility. Extensive experi-
022 ments on 14 benchmarks across 3 tasks, including Grounded VideoQA, Video
023 Temporal Grounding, and General VideoQA, demonstrate the effectiveness of the
024 proposed scheme in advancing video agent, test-time scaling, and long-form video
025 reasoning. Code, models, and data will be publicly available.
026

027 **1 INTRODUCTION**
028

029 Recent advancements in large language models (LLMs) have demonstrated remarkable success in
030 text-based reasoning (Wei et al., 2022; Yao et al., 2023a; Shinn et al., 2023), significantly improv-
031 ing both accuracy and interpretability in complex problem-solving scenarios (Yao et al., 2023b).
032 Following these breakthroughs, efforts have been devoted to extending these reasoning capabili-
033 ties to multi-modal domains (Zhang et al., 2023c; Xu et al., 2025; Thawakar et al., 2025) such as
034 vision-centric science (Lu et al., 2022) and math (Ma et al., 2025) understanding.
035

036 Among multi-modal signals, videos pose a unique challenge due to their temporal dimension, in-
037 troducing complexities absent in images or text. Effective video reasoning requires not only recog-
038 nizing visual appearances but also understanding how they evolve over time (Xiao et al., 2024; Di
039 & Xie, 2023; Chen et al., 2024a; Liu et al., 2024e; Wu et al., 2025). While recent visual Chain-of-
040 Thought (CoT) methods (Zhang et al., 2023c; Xu et al., 2025; Thawakar et al., 2025) excel at gener-
041 ating detailed thoughts for static images, they struggle with long videos as they cannot explicitly
042 localize or revisit earlier parts of the sequence, as presented in Figure 1 (left). Humans, by contrast,
043 can reason over long videos with ease: they break down complex problems, identify relevant mo-
044 ments, revisit them to confirm details, and synthesize their observations into coherent answers. This
045 natural proficiency motivates the development of an AI agent that emulates this process – flexibly
046 coordinating multiple capabilities to achieve advanced, vision-centric reasoning.
047

048 In this work, we introduce **VideoMind**, a video-language agent with enhanced temporal-grounded
049 reasoning capabilities. To meet the demands of diverse tasks, we define four essential roles for un-
050 derstanding complex long-form videos: (1) a **planner** to decompose tasks and coordinate other
051 roles, (2) a **grounder** for precise moment localization, (3) a **verifier** for moment candidates
052 assessment, and (4) an **answerer** for moment-aware response generation. Each role is carefully
053 designed to deliver strong performance, for example, the grounder is equipped with a timestamp
decoder to ensure accurate temporal grounding. To enable efficient integration of these roles, we
also propose a novel **Chain-of-LoRA** mechanism, where all the roles are implemented based on a

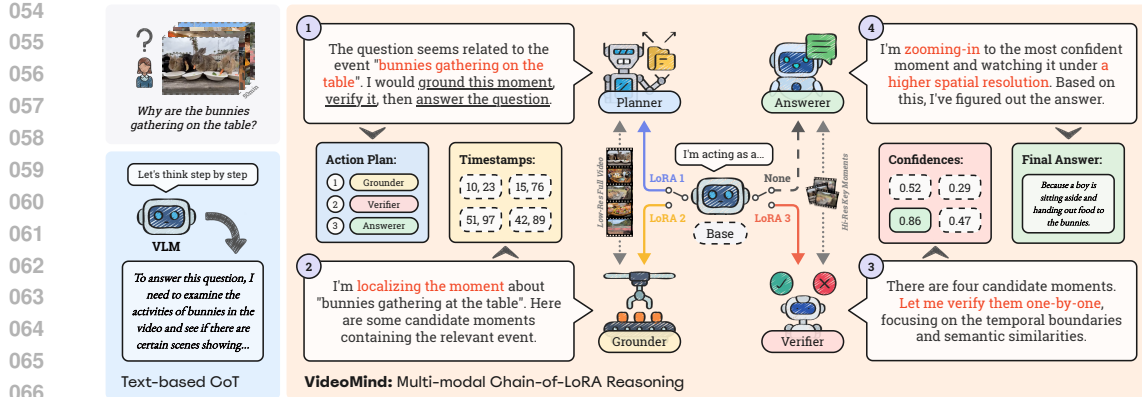


Figure 1: Illustration of VideoMind’s Chain-of-LoRA reasoning mechanism. The problem is decomposed by the planner and distributed to grounder, verifier, and answerer to systematically localize, verify, and interpret the relevant video moments.

unified LMM backbone with role-specific LoRA adapters (Hu et al., 2022). Therefore, role-specific capabilities can be trained separately on tailored datasets. During inference, all the LoRA parameters are cached into the memory, so that each role could be activated by simply switching to the corresponding LoRA, as shown in Figure 1 (right). This approach reflects a minimalist yet flexible design philosophy, facilitating seamless transitions and interactions among roles without incurring the memory overhead of maintaining multiple full models. As a result, VideoMind achieves both efficiency and flexibility on diverse video understanding tasks.

We conduct extensive experiments on 14 public benchmarks, including 3 on Grounded VideoQA, 6 on Video Temporal Grounding, and 5 on General VideoQA, to evaluate the effectiveness of our approach. VideoMind exhibits strong adaptability in addressing diverse reasoning tasks by jointly providing accurate responses and temporal-grounded evidence. Notably, our 2B model surpasses GPT-4o (OpenAI, 2024a) and Gemini-1.5-Pro (Reid et al., 2024) on several long video benchmarks such as CG-Bench (Chen et al., 2024a), MLVU (Zhou et al., 2024), and LVbench (Wang et al., 2024d). State-of-the-art performance is also achieved on temporal grounding datasets including QVHighlights (Lei et al., 2021) and Charades-STA (Gao et al., 2017). We further conduct ablation studies to justify our design choices, particularly the Chain-of-LoRA mechanism for enhancing flexibility while preserving efficiency. Our contributions are summarized as follows:

1. We propose **VideoMind**, a multi-modal agentic framework that enhances video reasoning by emulating human cognitive processes, including task decomposition, moment localization and verification, and answer synthesis. It addresses the unique challenges of long video reasoning in a progressive and structured manner.
2. We also introduce **Chain-of-LoRA**, an efficient test-time scaling mechanism that enables a single model to seamlessly switch among multiple roles. This approach enhances VideoMind’s flexibility without incurring additional memory overhead.
3. Our method demonstrates strong performance across three scenarios: Grounded VideoQA, Video Temporal Grounding, and General VideoQA. Notably, VideoMind-2B outperforms GPT-4o and Gemini-1.5-Pro on several long video benchmarks.

2 RELATED WORK

Temporal-grounded Video Understanding Significant advances in video understanding have propelled tasks such as video captioning (Zhao et al., 2023; Lin et al., 2024b), video question answering (Xiao et al., 2021; Zhang et al., 2023a), and video-text retrieval (Miech et al., 2019; Lin et al., 2022). However, these models often lack *visually grounded correspondence* and interpretability, particularly for long-form videos. The task of Video Temporal Grounding (Gao et al., 2017; Krishna et al., 2017) tackles this issue by requiring precise temporal localization for diverse queries, though regression-based models (Liu et al., 2022; 2024d) excel at localization but fall short in providing textual interpretability. Recent benchmarks (Xiao et al., 2024; Chen et al., 2024a; Liu et al.,

2024e) intensify this challenge, demanding both reasoning for complex questions and fine-grained temporal correspondence. Previous baselines for these tasks typically rely on multi-task objectives or modular agents composed of distinct components (Yu et al., 2023; Wang et al., 2024e; Fan et al., 2024), often yielding sub-optimal performance or overly complex systems, which constrain their efficiency and flexibility. Our VideoMind is an agentic workflow built upon a unified LMM, seamlessly integrating multiple functionalities while enhancing localization and interpretability, thus surpassing the limitations of prior methods.

Multi-modal Reasoning Large Multi-modal Models (Liu et al., 2023; 2025) exhibit generalized capabilities such as free-form question answering. However, they fall short in addressing complex challenges that often require reasoning (Wei et al., 2022). One approach to overcome this is to develop agent-based interfaces (Zhang et al., 2023a; Kahatapitiya et al., 2024), which integrates textual outputs from visual tools to enable reasoning via LLMs. Advanced methods (Suris et al., 2023; Yang et al., 2023; Gao et al., 2023) invoke visual APIs (*e.g.*, detectors and captioners) through progressive execution and reasoning. *Alternatively, pure text-based reasoning (OpenAI, 2024b; Guo et al., 2025) has been a dominant paradigm in LLMs, exemplified by training with long CoT processes using reinforcement learning, which provides detailed step-by-step reasoning, with some works (Zhang et al., 2023c; Xu et al., 2025; Chen et al., 2025b; Feng et al., 2025) extending this mechanism to the visual domain.* Despite these advances, extending reasoning to videos remains an open challenge. Given the long-context nature of informative videos, we believe that *a vision-centric* CoT should incorporate a human-like re-watching strategy and self-validation of intermediate observations, leading us to introduce a novel Chain-of-LoRA framework for video reasoning.

Inference-time Searching Inference-time searching has emerged as a critical technique for tackling complex reasoning and planning challenges in domains like robotics (Wang et al., 2023), games (Silver et al., 2016), and navigation (Teng et al., 2023). The advent of OpenAI o1 (OpenAI, 2024b) has advanced these inference-time techniques within LLMs by integrating sampling strategies such as controlled decoding (Chakraborty et al., 2024; Xu et al., 2024b), Best-of-N sampling (Lightman et al., 2023), and Monte Carlo Tree Search (MCTS) (Wang et al., 2024f; Zhang et al., 2024a; Wang et al., 2024a), allowing LLMs to iteratively refine outputs and achieve superior performance without altering their underlying weights. However, the potential of inference-time searching remains largely untapped in video understanding, where temporal reasoning introduces unique challenges. In our framework, we explore how such a strategy can be tailored for video temporal reasoning, observing that models are highly sensitive to the selection of temporal segments, often producing unreliable predictions when segment choices are sub-optimal. To address this, we propose a *moment-level* searching approach where a grounder generates multiple candidates, followed by a verifier that evaluates and determines the correct correspondence. *The framework also supports flexible inference-time role switching with minimal memory overhead.*

3 METHOD

Overview Figure 2 provides an overview of VideoMind. Our model derives from the Qwen2-VL (Wang et al., 2024c) architecture, consisting of an LLM backbone and a ViT-based visual encoder support dynamic resolution inputs. Given a video input \mathcal{V} and a text query \mathcal{Q} , the model performs step-by-step reasoning by adaptively calling different roles: (1) **Planner**: Dynamically coordinates the following roles based on the query. (2) **Grounder**: Identifies and localizes relevant video moments. (3) **Verifier**: Evaluates the validity of the moments identified by the grounder, refining them through a zoom-in process with boolean outputs. (4) **Answerer**: Generates the final response in natural language. This mechanism enables the models to **revisit the videos several times** (with varying temporal segments & spatial resolutions) to derive the final response.

3.1 PLANNER

An agent must be flexible enough to handle diverse tasks and efficiently determine which functions (roles) to call. To achieve this, we design the **planner**, which dynamically coordinates all the other roles for each query. It decides the sequence of function calls based on the multi-modal context. We utilize a JSON-style object `{"type": "<role>", "value": "<argument>"}` to denote a function call. In this way, a sequence of roles can be succinctly represented as a list of such objects. Three reasoning plans for different tasks are pre-defined and illustrated in Figure 3.

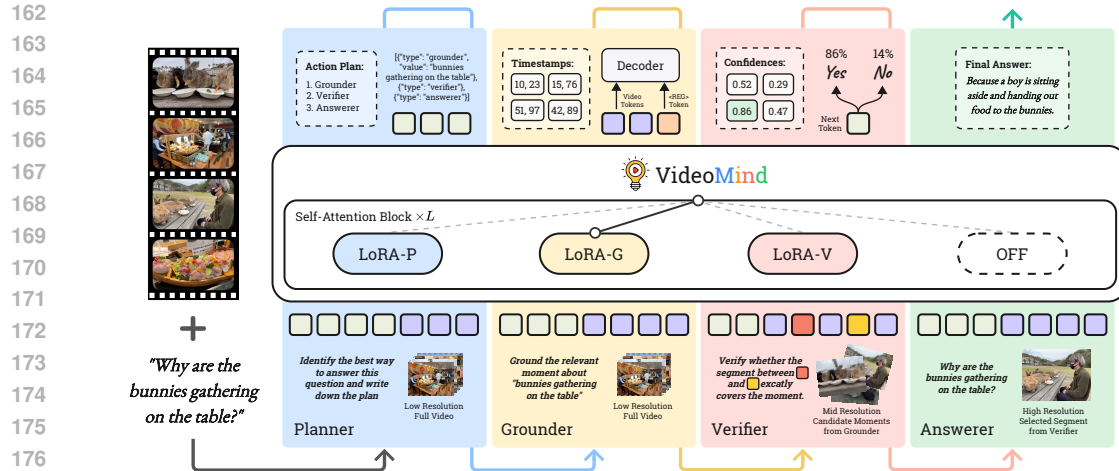


Figure 2: The overall workflow of VideoMind. Given a video and a query, it adaptively activates different roles (e.g., Planner \rightarrow Grounder \rightarrow Verifier \rightarrow Answerer in this case) and performs step-by-step reasoning by calling individual modules.

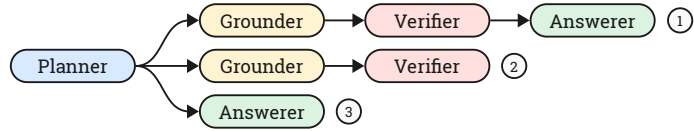


Figure 3: Planner coordinates all the other roles based on the video and query context, offering three reasoning plans and a query rephrasing mechanism to address diverse demands.

(1) Grounding & Verifying & Answering: This plan requires the agent to generate both a textual response and a corresponding temporal moment. For example, in Grounded VideoQA scenarios (Xiao et al., 2021), to answer the question “*What is the boy doing when the baby is crying?*”, the agent should identify the moment of “*baby is crying*”, and then investigate the boy’s activity.

(2) Grounding & Verifying: This plan is designed for grounding-only tasks such as moment retrieval (Lei et al., 2021; Gao et al., 2017). For questions like “*When does the woman go down-stairs?*”), the model should provide precise timestamps directly as the answer. Since the grounding results could potentially be unreliable, an extra zoom-in verification step is necessary.

(3) Answering Only: If the question is straightforward (e.g., “*Summarize this video*”) or the video is very short (e.g., less than 10s), it could be unnecessary to perform grounding. Instead, the model should watch the entire video and answer the question directly.

Query Rephrasing When the user query lacks sufficient detail for accurate moment localization, the planner is allowed to **rephrase** the question into a more descriptive version. For instance, the question “*What is the person sitting on the bed doing as the baby plays?*” may confuse the grounder as it contains multiple events (“*person sitting on the bed*” and “*baby plays*”). It can be rephrased to “*the baby is playing*” as an accurate scene description.

To train the planning and query rephrasing capabilities, we curated a dataset of 39K samples (shown in Table 1) from public benchmarks. For planning, we aligned each reasoning plan with corresponding question types: *temporal* questions from NExT-QA (Xiao et al., 2021) are assigned to Plan-1, moment queries from QVHighlights (Lei et al., 2021) are for Plan-2, and *causal & descriptive* questions from NExT-QA (Xiao et al., 2021) are for Plan-3. For query rephrasing, we leverage GPT-4o mini (OpenAI, 2024a) to generate synthetic video + question \rightarrow query samples for training.

3.2 GROUNDER

The **grounder** aims to localize relevant moments (*i.e.*, predicting start and end timestamps) based on text queries, thereby supporting the reasoning process by identifying visual cues. This requirement calls for the development of an LMM with robust temporal grounding capabilities.

216 **Timestamp Decoder** Instead of directly predicting timestamps through language modeling (Ren
 217 et al., 2024) or special tokens (Huang et al., 2024a; Liu et al., 2024e), we develop a timestamp
 218 decoder to maximize the LMM-based grounding performance. Specifically, we introduce a <REG>
 219 token to facilitate this process. When the <REG> token is generated, the last-layer hidden states of
 220 it and all the visual tokens will be sent into the decoder for timestamp prediction, obtaining a tuple
 221 $[t_{start}, t_{end}]$ representing the normalized start and end timestamps.

222 As shown in Figure 4, the decoder accepts the hidden states
 223 of the visual tokens $\mathbf{h}_v \in \mathbb{R}^{(T \times H \times W) \times D_L}$ and the <REG>
 224 token $\mathbf{h}_r \in \mathbb{R}^{1 \times D_L}$ as inputs, where T, H, W, D_L are the
 225 downsampled number of frames, height, width, and hidden
 226 dimensions of the LLM, respectively. We apply a 1D average
 227 pooling with kernel size and stride equal to $H \times W$ to
 228 compress the visual tokens to one token per frame.

$$\mathbf{h}'_v = \text{AvgPool}(\mathbf{h}_v) \in \mathbb{R}^{T \times D_L} \quad (1)$$

231 Then, \mathbf{h}'_v and \mathbf{h}_r are projected by two linear layers E_v and
 232 E_r to reduce the hidden dimension to D .

$$\mathbf{e}_v = E_v(\mathbf{h}'_v) \in \mathbb{R}^{T \times D}, \quad \mathbf{e}_r = E_r(\mathbf{h}_r) \in \mathbb{R}^{1 \times D} \quad (2)$$

233 The resulting \mathbf{e}_v and \mathbf{e}_r serve as consolidated representations
 234 of the video frames and the query¹, respectively. To
 235 effectively integrate their information, we concatenate them
 236 along the sequence dimension and send them into a three-
 237 layer transformer encoder (Vaswani et al., 2017).
 238

$$[\mathbf{e}'_v; \mathbf{e}'_r] = \text{Transformer}([\mathbf{e}_v + \mathbf{m}_v + \mathbf{e}_p; \mathbf{h}_r + \mathbf{m}_r]) \quad (3)$$

241 Here, modality indicators $\mathbf{m}_v \in \mathbb{R}^{1 \times D}$ and $\mathbf{m}_r \in \mathbb{R}^{1 \times D}$ are
 242 randomly initialized learnable embeddings. \mathbf{m}_v is expanded
 243 to $T \times D$ before being added with \mathbf{e}_v . \mathbf{e}_p is a normalized si-
 244 nusoidal positional encoding (Vaswani et al., 2017) for pre-
 245 serving temporal awareness. The output sequence is split
 246 back into \mathbf{e}'_v and \mathbf{e}'_r , indicating the contextualized frame and query
 247 embeddings, respectively.

248 **Temporal Feature Pyramid** To improve the model’s adaptability to videos and moments of vary-
 249 ing lengths, we map \mathbf{e}'_v into a four-level temporal feature pyramid (Liu et al., 2024d; Zhang et al.,
 250 2022). Each level is produced by a Conv1D \rightarrow LayerNorm \rightarrow SiLU block, where the Conv1D
 251 employs a kernel size and stride of 2. Therefore, the resulting four levels retain 1, 1/2, 1/4,
 252 and 1/8 of the original sequence length, respectively. To accelerate the prediction, we con-
 253 catenate the sequences from all pyramid levels along the temporal dimension to form \mathbf{p}_v with length
 $L = T + T/2 + T/4 + T/8$, allowing parallelized prediction across temporal resolutions.

254 **Prediction Heads** We introduce two heads for timestamps prediction: **(1) A classification head** is
 255 designed for frame-level foreground-background classification. This is instantiated by a two-layer
 256 Conv1D module with kernel size 3 and padding 1, followed by a Sigmoid activation. The outputs
 257 are frame-level confidence scores $\{\hat{c}_i\}_{i=0}^L$ indicating whether each frame falls inside the desired
 258 moment. A binary focal loss (Lin et al., 2017) is utilized to optimize these scores.

$$\mathcal{L}_{cls} = -\lambda_{cls} \alpha (1 - \hat{c}_i)^\gamma \log(\hat{c}_i) \quad (4)$$

261 Here, $\alpha = 0.9$ and $\gamma = 2.0$ are hyperparameters of the focal loss, and λ_{cls} is the loss reweighing
 262 term. **(2) A boundary regression head** is adopted to predict the frame-level temporal offsets for
 263 start and end boundaries $\{[\hat{b}_i^s, \hat{b}_i^e]\}_{i=0}^L$. This is also a two-layer Conv1D block (with 2 output
 264 channels), followed by an exponential activation. Predictions from different pyramid levels are further
 265 modulated by different learnable scaling factors. These outputs are supervised by an $L1$ loss.

$$\mathcal{L}_{reg} = \lambda_{reg} (|\hat{b}_i^s - b_i^s| + |\hat{b}_i^e - b_i^e|) \quad (5)$$

267 In order to realize better alignment between \mathbf{e}'_v and \mathbf{e}'_r , we incorporate an additional contrastive
 268 loss to encourage learning more discriminative representations. Specifically, we calculate the cosine

269 ¹We use the term “query” to denote the features of <REG> token.

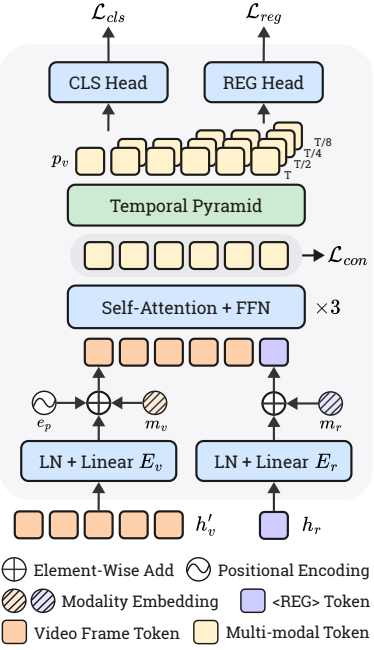


Figure 4: Detailed architecture of the timestamp decoder.

270

271
272
Table 1: Training datasets for different roles. Source datasets were repurposed for training planner
and verifier. mr and $step$ denote the moment retrieval and step localization subsets, respectively.

273

274

275

276

277

278

279

Role	#Samples	Source Datasets
Planner	39K	NeXT-QA (34K), QVHighlights (5K)
Grounder	210K	QVHighlights (5K), DiDeMo (33K), TACoS (9K), InternVid-VTime (54K), CosMo-Cap (87K), QuerYD (19K), HiREST _{mr} (8K), HiREST _{step} (4K)
Verifier	232K	DiDeMo (165K), TACoS (43K), QVHighlights (24K)

similarities among all frame-query pairs (denoted as $\{s_i\}_{i=0}^L$), then sample a positive frame (falling within the ground truth boundary) and apply the following optimization objective:

$$\mathcal{L}_{con} = -\lambda_{con} \log \frac{\exp(s_p/\tau)}{\exp(s_p/\tau) + \sum_{i \in \Theta} \exp(s_i/\tau)} \quad (6)$$

Here, Θ is the set of frame indices with $s_p > s_i$, and $\tau = 0.07$ is the temperature parameter. The final loss for the timestamp decoder is the sum of these losses at all layers with $\lambda_{cls} = 5.0$, $\lambda_{reg} = 1.0$, and $\lambda_{con} = 0.05$. The training datasets for the grounder are listed in Table 1.

3.3 VERIFIER

Key moments are crucial for providing visual cues, yet they might be unreliable due to grounding errors. Thus, further verifications are necessary. We let the grounder generate top-5 predictions, then employ the **Verifier** to select the most reliable one. This process is presented below.

Recap by Zooming-in For each candidate moment, we apply a zoom-in strategy by expanding the boundaries by 50% on both sides and temporally cropping the enlarged segment. The resulting segment and the original text query are sent to the verifier to assess whether the queried event exactly occurs within the temporal boundaries. To enhance boundary awareness, we adopt two special tokens, `<SEG-START>` and `<SEG-END>`, to explicitly mark the beginning and end of the moment. These tokens are inserted among the visual tokens at the corresponding frames, effectively guiding the model in recognizing moment boundaries.

Boolean Judgement The verifier’s responses are binary, *i.e.*, either “Yes” or “No”. To train this role, we sample predictions from the grounder and assign binary labels based on an IoU threshold of 0.5. The model is then fine-tuned via SFT to predict these labels. During inference, for each candidate moment, we employ teacher forcing to obtain the likelihoods of the `<Yes>` and `<No>` tokens, denoted as L_y and L_n , respectively. The confidence score is then computed as $\text{Sigmoid}(L_y - L_n)$. The moment with the highest score is selected and passed to the answerer.

3.4 ANSWERER

The **answerer** responds to the given question based on the cropped video segment (w/ grounder) or the whole video (w/o grounder). Since the objective of this role is strictly aligned with existing LMMs, we employ the original model directly *without fine-tuning or architectural modifications*.

3.5 CHAIN-OF-LORA

The four roles introduced above demonstrate distinct yet complementary capabilities, collaborating to achieve advanced vision-centric reasoning. However, simply integrating these roles into a single model poses challenges, as their core functionalities can interfere with one another. To avoid inefficiently implementing them as multiple models while still accommodating diverse demands, we propose a novel **Chain-of-LoRA** mechanism to enable flexible and efficient role switching.

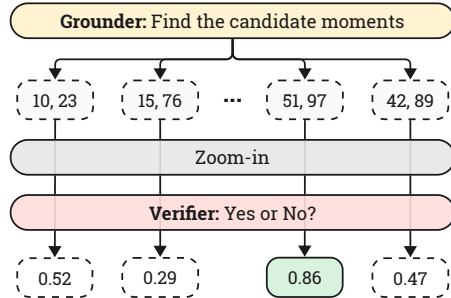


Figure 5: The grounder generates multiple candidate moments, which are then refined by the verifier via **zooming-in** to investigate and select the best one.

324

325

Table 2: Performance comparison on Grounded VideoQA on CG-Bench (Chen et al., 2024a).

326

327

Method	Size	long-acc.	mIoU	rec. @ IoU	acc. @ IoU
GPT-4o (OpenAI, 2024a)	–	45.2	5.62	8.30	4.38
Gemini-1.5-Pro (Reid et al., 2024)	–	37.2	3.95	5.81	2.53
Claude-3.5-Sonnet (Anthropic, 2025)	–	40.5	3.99	5.67	2.79
Video-LLaVA (Lin et al., 2023a)	7B	16.2	1.13	1.96	0.59
VideoLLaMA (Zhang et al., 2023b)	7B	18.4	1.21	1.87	0.84
VideoChat2 (Li et al., 2024b)	7B	19.3	1.28	1.98	0.94
ST-LLM (Liu et al., 2024c)	7B	23.8	2.23	2.86	1.13
ShareGPT4Video (Chen et al., 2024c)	16B	26.7	1.85	2.65	1.01
Chat-UniVi-v1.5 (Jin et al., 2023)	13B	25.9	2.07	2.53	1.21
VILA (Lin et al., 2024a)	8B	28.7	1.56	2.89	1.35
Long VA (Zhang et al., 2024b)	7B	28.7	2.94	3.86	1.78
LLaVA-OneVision (Li et al., 2024a)	7B	31.1	1.63	1.78	1.08
Video-CCAM (Fei et al., 2024)	14B	29.7	2.63	3.48	1.83
Kangaroo (Liu et al., 2024b)	8B	30.2	2.56	2.81	1.94
VITA (Fu et al., 2024b)	8×7B	33.3	3.06	3.53	2.06
Qwen2-VL (Wang et al., 2024c)	72B	41.3	3.58	5.32	3.31
InternVL2 (OpenGVLab, 2024)	78B	42.2	3.91	5.05	2.64
VideoMind (Ours)	2B	31.0	<u>5.94</u>	<u>8.50</u>	4.02
VideoMind (Ours)	7B	38.4	7.10	9.93	4.67

328

329

330

331

332

333

334

335

336

337

338

339

340

341

342

343

Table 3: Performance comparison on Grounded VideoQA on ReXTime (Chen et al., 2024b). FT indicates fine-tuning on the target dataset.

344

Method	Size	FT	R@0.3	R@0.5	mIoU	Acc	Acc@IoU
VTimeLLM (Huang et al., 2024a)	7B	✗	28.84	17.41	20.14	36.16	–
TimeChat (Ren et al., 2024)	7B	✗	14.42	7.61	11.65	40.04	–
LITA (Huang et al., 2024b)	13B	✗	29.49	16.29	21.49	34.44	–
VTimeLLM (Huang et al., 2024a)	7B	✓	43.69	26.13	29.92	57.58	17.13
TimeChat (Ren et al., 2024)	7B	✓	40.13	21.42	26.29	49.46	10.92
VideoMind (Ours)	2B	✗	<u>34.31</u>	<u>22.69</u>	<u>24.83</u>	<u>69.06</u>	<u>17.26</u>
VideoMind (Ours)	7B	✗	38.22	25.52	27.61	74.59	20.20

345

346

347

348

349

350

351

352

353

354

355

356

357

358

359

In greater detail, all roles are based on a shared LMM backbone and are augmented with different LoRA adapters (Hu et al., 2022). Note that an additional timestamp decoder is used exclusively by the grounder. During inference, the framework dynamically activates role-specific LoRA adapters according to the planner, thereby maximizing the strengths of each role while minimizing the memory consumption and architectural modifications to the base model.

4 EXPERIMENTS

We evaluate the effectiveness of VideoMind through extensive experiments across 14 public benchmarks. Specifically, we study the following research questions.

- Q1.** Whether VideoMind is flexible and effective on diverse video understanding tasks compared to the corresponding baselines with task-specific designs?
- Q2.** Compared with (1) training a single agent on multiple tasks or (2) distributing all roles to different models, what advantages does Chain-of-LoRA offer?
- Q3.** What effects does each individual design contribute? More importantly, whether each role is necessary for building such a video reasoning system?

Detailed information about the benchmarks, evaluation settings, implementation details, and more experimental results can be found in the appendix.

4.1 Q1: COMPARISON WITH STATE-OF-THE-ARTS

Grounded Video Question Answering Table 2 compares the Grounded VideoQA performance on CG-Bench (Chen et al., 2024a), a challenging video benchmark with an average duration of 27 minutes. On temporal grounding metrics (mIoU and rec. @ IoU), our lightweight 2B model outperforms all the baselines, including GPT-4o (OpenAI, 2024a) and Gemini 1.5 Pro (Reid et al., 2024). Our 7B model further setups a new state-of-the-art on clue-grounded QA (acc. @ IoU). In Table 3 and Table 4, we further present the comparison results on ReXTime (Chen et al., 2024b) and NExT-GQA

378

379

Table 4: Performance comparison on Grounded VideoQA on NExT-GQA (Xiao et al., 2024).

380

381

382

383

384

385

386

387

388

389

Method	Size	IoU			IoP			Acc@GQA
		R@0.3	R@0.5	mIoU	R@0.3	R@0.5	mIoP	
FrozenBiLM NG+ (Yang et al., 2022)	890M	13.5	6.1	9.6	28.5	23.7	24.2	17.5
SeViLA (Yu et al., 2023)	4B	29.2	13.8	21.7	34.7	22.9	29.5	16.6
LangRepo (Kahatapitiya et al., 2024)	8×7B	—	12.2	18.5	—	28.7	31.3	17.1
VideoStreaming (Qian et al., 2024b)	8.3B	—	13.3	19.3	—	31.0	32.2	17.8
LLoVi (Zhang et al., 2023a)	1.8T	—	15.3	20.0	—	36.9	37.3	24.3
HawkEye (Wang et al., 2024g)	7B	37.0	19.5	25.7	—	—	—	—
VideoChat-TPO (Yan et al., 2024)	7B	41.2	<u>23.4</u>	27.7	47.5	32.8	35.6	<u>25.5</u>
VideoMind (Ours)	2B	45.2	23.2	28.6	51.3	32.6	36.4	25.2
VideoMind (Ours)	7B	50.2	25.8	31.4	56.0	<u>35.3</u>	39.0	28.2

390

391

392

Table 5: Performance comparison on video temporal grounding on Charades-STA (Gao et al., 2017) and ActivityNet-Captions (Krishna et al., 2017). FT means fine-tuning on the target dataset.

393

394

395

396

397

398

399

400

401

402

403

Method	Size	FT	Charades-STA				ActivityNet-Captions			
			R@0.3	R@0.5	R@0.7	mIoU	R@0.3	R@0.5	R@0.7	mIoU
VTimeLLM (Huang et al., 2024a)	7B	✗	51.0	27.5	11.4	31.2	44.0	27.8	14.3	30.4
TimeChat (Ren et al., 2024)	7B	✗	51.5	32.2	13.4	—	—	—	—	—
Momentor (Qian et al., 2024a)	7B	✗	42.6	26.6	11.6	28.5	42.9	23.0	12.4	29.3
ChatVTG (Qu et al., 2024)	7B	✗	52.7	33.0	15.9	34.9	40.7	22.5	9.4	27.2
VideoChat-TPO (Yan et al., 2024)	7B	✗	58.3	40.2	18.4	38.1	—	—	—	—
E.T. Chat (Liu et al., 2024e)	4B	✗	65.7	45.9	20.0	42.3	24.1	12.8	6.1	18.9
Grounded-VideoLLM (Wang et al., 2024b)	4B	✗	54.2	36.4	19.7	36.8	—	—	—	—
TRACE (Guo et al., 2024)	7B	✗	—	40.3	19.4	—	—	—	—	—
LLaVA-ST (Li et al., 2025a)	7B	✗	63.1	44.8	23.4	42.4	—	—	—	—
UniTime (Li et al., 2025b)	7B	✗	—	59.1	31.9	52.2	—	22.8	14.1	27.3
VideoMind (Ours)	2B	✗	67.6	51.1	26.0	45.2	44.0	26.5	12.6	30.1
VideoMind (Ours)	7B	✗	73.5	59.1	<u>31.2</u>	<u>50.2</u>	48.4	30.3	15.7	33.3

404

405

406

407

Table 6: Performance comparison on General VideoQA on Video-MME (Fu et al., 2024a), MLVU (Zhou et al., 2024), and LVBench (Wang et al., 2024d).

408

409

410

411

412

413

414

415

416

417

Method	Size	Video-MME		MLVU	LVBench
		All	Long	M-Avg	Overall
GPT-4o (OpenAI, 2024a)	—	71.9	65.3	54.5	30.8
Gemini-1.5-Pro (Reid et al., 2024)	—	75.0	67.4	—	33.1
Video-LLaVA (Lin et al., 2023a)	7B	41.1	37.8	29.3	—
TimeChat (Ren et al., 2024)	7B	34.3	32.1	30.9	22.3
MovieChat (Song et al., 2023)	7B	38.2	33.4	25.8	22.5
PLLaVA (Xu et al., 2024a)	34B	40.0	34.7	53.6	26.1
VideoChat-TPO (Yan et al., 2024)	7B	48.8	41.0	54.7	—
LongVA (Zhang et al., 2024b)	7B	52.6	46.2	56.3	—
VideoMind (Ours)	2B	55.4	46.3	58.7	35.4
VideoMind (Ours)	7B	58.2	49.2	64.4	40.8

418

Video Temporal Grounding We also evaluate the grounder and verifier on video temporal grounding datasets. The results on Charades-STA (Gao et al., 2017) and ActivityNet-Captions (Krishna et al., 2017) are shown in Table 5. Benefiting from (1) the timestamp decoder design, and (2) a verifier that refines the results by focusing on critical segments, our model surpasses all LLM-based temporal grounding methods and yields competitive results compared to fine-tuned experts.

424

425

426

427

General Video Question Answering We are also interested in whether our temporally augmented design can improve general VideoQA tasks. In Table 6, we evaluate our model on three long video benchmarks to determine if the Chain-of-LoRA design generalizes to common settings. Our designs effectively help the model localize cue segments before answering the question.

428

429

4.2 Q2: THE ADVANTAGES OF CHAIN-OF-LORA

430

431

Table 7 studies the effect of role integration on VideoMind-2B. First, text-based CoT does not improve the base model, highlighting the need for a vision-centric reasoning strategy. Second, the key capabilities of roles may conflict with one another, thus only sub-optimal performance can be

(Xiao et al., 2024). Despite the challenges posed by the causal event relationships on ReXTime, our model can successfully identify the correct moment, resulting in significant performance boosts compared with zero-shot baselines. On NExT-GQA, compared to agent-based solutions such as LLoVi (Zhang et al., 2023a) and LangRepo (Kahatapitiya et al., 2024) and end-to-end methods like VideoChat-TPO (Yan et al., 2024), VideoMind demonstrates its effectiveness on both key event grounding and question answering.

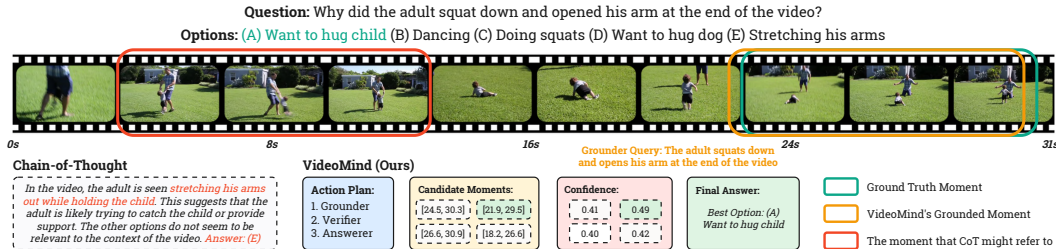


Figure 6: Visualization of the reasoning process of VideoMind. Through chaining the planner, groundner, verifier, and answerer, our model accurately localizes the critical moment and selects the correct answer, avoiding confusion from incorrect segments.

Table 7: Performance and efficiency comparison of different test-time scaling and role integration strategies. Mem indicates the peak GPU memory consumption. Notably, Chain-of-LoRA achieves the best performance with minimal memory cost.

Table 8: Effects of individual roles. A, G, V, P, G% denote the answerer, grounder, verifier, planner, and the percentage of samples processed with the grounder, respectively.

Method	Mem	NExT-GQA		Charades-STA		Video-MME	
		mIoU	Acc	R@0.5	mIoU	All	Long
Qwen2-VL-2B + CoT	4.1G	—	69.6	—	—	53.0	43.1
	4.1G	—	69.7	—	—	52.8	43.3
+ All-in-One	4.2G	28.0	70.5	47.8	42.1	53.6	43.6
+ All-Distributed	16.6G	28.6	71.4	51.1	45.2	55.4	46.3
+ Chain-of-LoRA	4.2G	28.6	71.4	51.1	45.2	55.4	46.3

achieved via joint training. Compared to the all-distributed approach that requires multiple copies ($4\times$) of weights, Chain-of-LoRA offers the best balance between effectiveness and efficiency.

4.3 Q3: KEY ABLATION STUDIES

Effect of Individual Roles The contributions of different roles are studied in Table 8. Our observations are as follows: (1) **Grounder**: By identifying visual cues, the grounder can slightly improve QA accuracy, indicating that the grounder is especially effective on long videos. (2) **Verifier**: Selecting the best candidate through the verifier improves grounding performance, yielding a consistent gain of 3.2 mIoU on Charades-STA. (3) **Planner**: Coordinating roles via the planner – even when performing grounding on only 40% samples (the remaining 60% are directly processed by the answerer) – boosts the accuracy from 69.2 to 70.0. This highlights the model’s flexibility to adaptively determine whether to perform grounding under different temporal contexts.

4.4 VISUALIZATION

In Figure 6, we illustrate how VideoMind applies all roles to progressively derive the correct answer while avoiding potential mistakes. The planner determines what roles are needed, then calls the grounder to generate candidate moments. The verifier selects the most relevant segment (highlighted in yellow), which is then zoomed-in and passed to the answerer for further reasoning.

5 CONCLUSION

In this work, we introduced **VideoMind**, a video-language agent designed for temporal-grounded video reasoning. Our approach employs an agentic workflow consisting of four carefully designed roles along with a **Chain-of-LoRA** strategy to flexibly switch among them. Extensive experiments on Grounded VideoQA, Video Temporal Grounding, and General VideoQA tasks demonstrate the effectiveness and significance of our method, particularly in long-form video reasoning by providing evidence-based answers. We hope this work inspires future advancements in agentic reasoning.

Limitations & Future Work We acknowledge that our method requires careful optimization of individual designs and preparation of training data. In our future work, we will investigate (1) the possibility of joint-optimization of multiple roles and (2) the integration of audio modality.

486 ETHICS STATEMENT
487488 This study focuses on algorithmic innovations for improving the visual reasoning capabilities of
489 large multi-modal models. It does not involve human subjects, private data, or any potentially harmful
490 insights. All datasets used are publicly available and widely adopted in the community. We
491 acknowledge the potential risks of misuse associated with LLMs and LMMs, including the bias
492 propagation and harmful content generation. However, this study does not directly address the de-
493 ployment or generation. Instead, it contributes to the understanding of the model architecture and
494 the reasoning mechanism. To the best of our knowledge, our research complies with the ICLR Code
495 of Ethics and does not involve any known violations or harms.
496497 REPRODUCIBILITY STATEMENT
498499 We are committed to ensuring the full reproducibility of this study. To achieve this, we have pro-
500 vided key hyperparameters settings in Section 3, formulation of inference pipeline in Section A.1,
501 implementation details in Section A.2, evaluation metrics in Section B.1, and prompt templates in
502 Section C.1. We also open-source all the code (submitted as the supplementary material), model
503 checkpoints, data, and training logs in this study to facilitate future research in this direction.
504505 REFERENCES
506507 Marah Abdin, Sam Ade Jacobs, Ammar Ahmad Awan, Jyoti Aneja, Ahmed Awadallah, Hany
508 Awadalla, Nguyen Bach, Amit Bahree, Arash Bakhtiari, Harkirat Behl, et al. Phi-3 technical
509 report: A highly capable language model locally on your phone. *arXiv:2404.14219*, 2024.510 Josh Achiam, Steven Adler, Sandhini Agarwal, Lama Ahmad, Ilge Akkaya, Florencia Leoni Ale-
511 man, Diogo Almeida, Janko Altenschmidt, Sam Altman, Shyamal Anadkat, et al. Gpt-4 technical
512 report. *arXiv:2303.08774*, 2023.
513514 Anthropic. Claude 3.5 sonnet model card, 2025. URL <https://www.anthropic.com/news/claude-3-5-sonnet>.
515516 Shuai Bai, Keqin Chen, Xuejing Liu, Jialin Wang, Wenbin Ge, Sibo Song, Kai Dang, Peng Wang,
517 Shijie Wang, Jun Tang, et al. Qwen2.5-vl technical report. *arXiv:2502.13923*, 2025.
518519 Souradip Chakraborty, Soumya Suvra Ghosal, Ming Yin, Dinesh Manocha, Mengdi Wang, Am-
520 rit Singh Bedi, and Furong Huang. Transfer q star: Principled decoding for llm alignment.
521 *arXiv:2405.20495*, 2024.
522523 Guo Chen, Yicheng Liu, Yifei Huang, Yuping He, Baoqi Pei, Jilan Xu, Yali Wang, Tong Lu, and
524 Limin Wang. Cg-bench: Clue-grounded question answering benchmark for long video under-
525 standing. *arXiv:2412.12075*, 2024a.
526527 Jr-Jen Chen, Yu-Chien Liao, Hsi-Che Lin, Yu-Chu Yu, Yen-Chun Chen, and Frank Wang. Rextime:
528 A benchmark suite for reasoning-across-time in videos. In *NeurIPS*, pp. 28662–28673, 2024b.
529530 Lin Chen, Xilin Wei, Jinsong Li, Xiaoyi Dong, Pan Zhang, Yuhang Zang, Zehui Chen, Haodong
531 Duan, Zhenyu Tang, Li Yuan, et al. Sharegpt4video: Improving video understanding and genera-
532 tion with better captions. In *NeurIPS*, pp. 19472–19495, 2024c.
533534 Qirui Chen, Shangzhe Di, and Weidi Xie. Grounded multi-hop videoqa in long-form egocentric
535 videos. In *AAAI*, pp. 2159–2167, 2025a.
536537 Shimin Chen, Xiaohan Lan, Yitian Yuan, Zequn Jie, and Lin Ma. Timemarker: A versatile
538 video-llm for long and short video understanding with superior temporal localization ability.
539 *arXiv:2411.18211*, 2024d.
540541 Yukang Chen, Wei Huang, Baifeng Shi, Qinghao Hu, Hanrong Ye, Ligeng Zhu, Zhijian Liu, Pavlo
542 Molchanov, Jan Kautz, Xiaojuan Qi, et al. Scaling rl to long videos. *arXiv:2507.07966*, 2025b.
543

- 540 Google DeepMind. Gemini 2.5: Our most intelligent ai model, 2025. URL <https://blog.google/technology/google-deepmind/gemini-model-thinking-updates-march-2025/>.
- 541
- 542
- 543
- 544 Shangzhe Di and Weidi Xie. Grounded question-answering in long egocentric videos. *arXiv:2312.06505*, 2023.
- 545
- 546
- 547 Yue Fan, Xiaojian Ma, Rujie Wu, Yuntao Du, Jiaqi Li, Zhi Gao, and Qing Li. Videoagent: A
- 548 memory-augmented multimodal agent for video understanding. *arXiv:2403.11481*, 2024.
- 549
- 550 Jiajun Fei, Dian Li, Zhidong Deng, Zekun Wang, Gang Liu, and Hui Wang. Video-ccam: Enhanc-
- 551 ing video-language understanding with causal cross-attention masks for short and long videos.
- 552
- 553 *arXiv:2408.14023*, 2024.
- 554
- 555 Kaituo Feng, Kaixiong Gong, Bohao Li, Zonghao Guo, Yibing Wang, Tianshuo Peng, Junfei Wu,
- 556 Xiaoying Zhang, Benyou Wang, and Xiangyu Yue. Video-r1: Reinforcing video reasoning in
- 557 llmms. *arXiv:2503.21776*, 2025.
- 558
- 559 Chaoyou Fu, Yuhang Dai, Yongdong Luo, Lei Li, Shuhuai Ren, Renrui Zhang, Zihan Wang, Chenyu
- 560 Zhou, Yunhang Shen, Mengdan Zhang, et al. Video-mme: The first-ever comprehensive evalua-
- 561 tion benchmark of multi-modal llms in video analysis. *arXiv:2405.21075*, 2024a.
- 562
- 563 Chaoyou Fu, Haojia Lin, Zuwei Long, Yunhang Shen, Yuhang Dai, Meng Zhao, Yi-Fan Zhang,
- 564 Shaoqi Dong, Yangze Li, Xiong Wang, et al. Vita: Towards open-source interactive omni multi-
- 565 modal llm. *arXiv:2408.05211*, 2024b.
- 566
- 567 Difei Gao, Lei Ji, Luowei Zhou, Kevin Qinghong Lin, Joya Chen, Zihan Fan, and Mike Zheng
- 568 Shou. Assistgpt: A general multi-modal assistant that can plan, execute, inspect, and learn.
- 569
- 570 *arXiv:2306.08640*, 2023.
- 571
- 572 Jiyang Gao, Chen Sun, Zhenheng Yang, and Ram Nevatia. Tall: Temporal activity localization via
- 573 language query. In *ICCV*, pp. 5267–5275, 2017.
- 574
- 575 Kristen Grauman, Andrew Westbury, Eugene Byrne, Zachary Chavis, Antonino Furnari, Rohit Gird-
- 576 har, Jackson Hamburger, Hao Jiang, Miao Liu, Xingyu Liu, et al. Ego4d: Around the world in
- 577 3,000 hours of egocentric video. In *CVPR*, pp. 18995–19012, 2022.
- 578
- 579 Daya Guo, Dejian Yang, Haowei Zhang, Junxiao Song, Ruoyu Zhang, Runxin Xu, Qihao Zhu,
- 580 Shirong Ma, Peiyi Wang, Xiao Bi, et al. Deepseek-r1: Incentivizing reasoning capability in llms
- 581 via reinforcement learning. *arXiv:2501.12948*, 2025.
- 582
- 583 Yongxin Guo, Jingyu Liu, Mingda Li, Qingbin Liu, Xi Chen, and Xiaoying Tang. Trace: Temporal
- 584 grounding video llm via causal event modeling. *arXiv:2410.05643*, 2024.
- 585
- 586 Edward J Hu, Yelong Shen, Phillip Wallis, Zeyuan Allen-Zhu, Yuanzhi Li, Shean Wang, Lu Wang,
- 587 Weizhu Chen, et al. Lora: Low-rank adaptation of large language models. *ICLR*, 2022.
- 588
- 589 Bin Huang, Xin Wang, Hong Chen, Zihan Song, and Wenwu Zhu. Vtimellm: Empower llm to grasp
- 590 video moments. In *CVPR*, pp. 14271–14280, 2024a.
- 591
- 592 De-An Huang, Shijia Liao, Subhashree Radhakrishnan, Hongxu Yin, Pavlo Molchanov, Zhiding
- 593 Yu, and Jan Kautz. Lita: Language instructed temporal-localization assistant. *arXiv:2403.19046*,
- 594 2024b.
- 595
- 596 Dongfu Jiang, Xuan He, Huaye Zeng, Cong Wei, Max Ku, Qian Liu, and Wenhui Chen. Mantis:
- 597 Interleaved multi-image instruction tuning. *arXiv:2405.01483*, 2024.
- 598
- 599 Peng Jin, Ryuichi Takanobu, Caiwan Zhang, Xiaochun Cao, and Li Yuan. Chat-univi: Unified
- 600 visual representation empowers large language models with image and video understanding.
- 601 *arXiv:2311.08046*, 2023.
- 602
- 603 Kumara Kahatapitiya, Kanchana Ranasinghe, Jongwoo Park, and Michael S Ryoo. Language repos-
- 604 itory for long video understanding. *arXiv:2403.14622*, 2024.

- 594 Ranjay Krishna, Kenji Hata, Frederic Ren, Li Fei-Fei, and Juan Carlos Niebles. Dense-captioning
 595 events in videos. In *ICCV*, pp. 706–715, 2017.
- 596
- 597 Hugo Laurencon, Leo Tronchon, Matthieu Cord, and Victor Sanh. What matters when building
 598 vision-language models? In *NeurIPS*, pp. 87874–87907, 2024.
- 599
- 600 Jie Lei, Licheng Yu, Tamara L Berg, and Mohit Bansal. Tvr: A large-scale dataset for video-subtitle
 601 moment retrieval. In *ECCV*, pp. 447–463, 2020.
- 602
- 603 Jie Lei, Tamara L Berg, and Mohit Bansal. Qvhighlights: Detecting moments and highlights in
 604 videos via natural language queries. In *NeurIPS*, 2021.
- 605
- 606 Bo Li, Yuanhan Zhang, Dong Guo, Renrui Zhang, Feng Li, Hao Zhang, Kaichen Zhang, Peiyuan
 607 Zhang, Yanwei Li, Ziwei Liu, et al. Llava-onevision: Easy visual task transfer. *arXiv:2408.03326*,
 608 2024a.
- 609
- 610 Hongyu Li, Jinyu Chen, Ziyu Wei, Shaofei Huang, Tianrui Hui, Jialin Gao, Xiaoming Wei, and
 611 Si Liu. Llava-st: A multimodal large language model for fine-grained spatial-temporal under-
 612 standing. In *CVPR*, pp. 8592–8603, 2025a.
- 613
- 614 Kunchang Li, Yinan He, Yi Wang, Yizhuo Li, Wenhui Wang, Ping Luo, Yali Wang, Limin Wang,
 615 and Yu Qiao. Videochat: Chat-centric video understanding. *arXiv:2305.06355*, 2023a.
- 616
- 617 Kunchang Li, Yali Wang, Yinan He, Yizhuo Li, Yi Wang, Yi Liu, Zun Wang, Jilan Xu, Guo Chen,
 618 Ping Luo, et al. Mvbench: A comprehensive multi-modal video understanding benchmark. In
 619 *CVPR*, pp. 22195–22206, 2024b.
- 620
- 621 Pandeng Li, Chen-Wei Xie, Hongtao Xie, Liming Zhao, Lei Zhang, Yun Zheng, Deli Zhao, and
 622 Yongdong Zhang. Momentdiff: Generative video moment retrieval from random to real. In
 623 *NeurIPS*, pp. 65948–65966, 2023b.
- 624
- 625 Zeqian Li, Shangzhe Di, Zhonghua Zhai, Weilin Huang, Yanfeng Wang, and Weidi Xie.
 626 Universal video temporal grounding with generative multi-modal large language models.
 627 *arXiv:2506.18883*, 2025b.
- 628
- 629 Hunter Lightman, Vineet Kosaraju, Yuri Burda, Harrison Edwards, Bowen Baker, Teddy Lee, Jan
 630 Leike, John Schulman, Ilya Sutskever, and Karl Cobbe. Let’s verify step by step. In *ICLR*, 2023.
- 631
- 632 Bin Lin, Bin Zhu, Yang Ye, Munan Ning, Peng Jin, and Li Yuan. Video-llava: Learning united
 633 visual representation by alignment before projection. *arXiv:2311.10122*, 2023a.
- 634
- 635 Ji Lin, Hongxu Yin, Wei Ping, Pavlo Molchanov, Mohammad Shoeybi, and Song Han. Vila: On
 636 pre-training for visual language models. In *CVPR*, pp. 26689–26699, 2024a.
- 637
- 638 Kevin Qinghong Lin, Jinpeng Wang, Mattia Soldan, Michael Wray, Rui Yan, Eric Z Xu, Difei Gao,
 639 Rong-Cheng Tu, Wenzhe Zhao, Weijie Kong, et al. Egocentric video-language pretraining. In
 640 *NeurIPS*, pp. 7575–7586, 2022.
- 641
- 642 Kevin Qinghong Lin, Pengchuan Zhang, Joya Chen, Shraman Pramanick, Difei Gao, Alex Jin-
 643 peng Wang, Rui Yan, and Mike Zheng Shou. Univtg: Towards unified video-language temporal
 644 grounding. In *CVPR*, pp. 2794–2804, 2023b.
- 645
- 646 Kevin Qinghong Lin, Pengchuan Zhang, Difei Gao, Xide Xia, Joya Chen, Ziteng Gao, Jinheng
 647 Xie, Xuhong Xiao, and Mike Zheng Shou. Learning video context as interleaved multimodal
 648 sequences. In *ECCV*, pp. 375–396, 2024b.
- 649
- 650 Tsung-Yi Lin, Priya Goyal, Ross Girshick, Kaiming He, and Piotr Dollár. Focal loss for dense object
 651 detection. In *ICCV*, pp. 2980–2988, 2017.
- 652
- 653 Haotian Liu, Chunyuan Li, Qingyang Wu, and Yong Jae Lee. Visual instruction tuning. In *NeurIPS*,
 654 pp. 34892–34916, 2023.
- 655
- 656 Haotian Liu, Chunyuan Li, Yuheng Li, Bo Li, Yuanhan Zhang, Sheng Shen, and Yong Jae Lee.
 657 Llava-next: Improved reasoning, ocr, and world knowledge, 2024a. URL <https://llava-v1.github.io/blog/2024-01-30-llava-next/>.

- 648 Jiajun Liu, Yibing Wang, Hanghang Ma, Xiaoping Wu, Xiaoqi Ma, Xiaoming Wei, Jianbin Jiao,
 649 Enhua Wu, and Jie Hu. Kangaroo: A powerful video-language model supporting long-context
 650 video input. *arXiv:2408.15542*, 2024b.
- 651 Ruyang Liu, Chen Li, Haoran Tang, Yixiao Ge, Ying Shan, and Ge Li. St-llm: Large language
 652 models are effective temporal learners. In *ECCV*, pp. 1–18, 2024c.
- 654 Ye Liu, Siyuan Li, Yang Wu, Chang Wen Chen, Ying Shan, and Xiaohu Qie. Umt: Unified multi-
 655 modal transformers for joint video moment retrieval and highlight detection. In *CVPR*, pp. 3042–
 656 3051, 2022.
- 657 Ye Liu, Jixuan He, Wanhua Li, Junsik Kim, Donglai Wei, Hanspeter Pfister, and Chang Wen Chen.
 658 r^2 -tuning: Efficient image-to-video transfer learning for video temporal grounding. In *ECCV*,
 659 2024d.
- 661 Ye Liu, Zongyang Ma, Zhongang Qi, Yang Wu, Ying Shan, and Chang W Chen. E.t. bench: Towards
 662 open-ended event-level video-language understanding. In *NeurIPS*, pp. 32076–32110, 2024e.
- 664 Ye Liu, Zongyang Ma, Junfu Pu, Zhongang Qi, Yang Wu, Shan Ying, and Chang Wen Chen. Unip-
 665 ixel: Unified object referring and segmentation for pixel-level visual reasoning. In *NeurIPS*,
 666 2025.
- 667 Ilya Loshchilov and Frank Hutter. Decoupled weight decay regularization. In *ICLR*, 2019.
- 668 Pan Lu, Swaroop Mishra, Tanglin Xia, Liang Qiu, Kai-Wei Chang, Song-Chun Zhu, Oyvind Tafjord,
 669 Peter Clark, and Ashwin Kalyan. Learn to explain: Multimodal reasoning via thought chains for
 670 science question answering. In *NeurIPS*, pp. 2507–2521, 2022.
- 672 Zongyang Ma, Yuxin Chen, Ziqi Zhang, Zhongang Qi, Chunfeng Yuan, Shaojie Zhu, Chengxiang
 673 Zhuo, Bing Li, Ye Liu, Zang Li, Ying Shan, and Weiming Hu. Visionmath: Vision-form mathe-
 674 matical problem-solving. In *ICCV*, 2025.
- 676 Muhammad Maaz, Hanoona Rasheed, Salman Khan, and Fahad Shahbaz Khan. Video-chatgpt:
 677 Towards detailed video understanding via large vision and language models. *arXiv:2306.05424*,
 678 2023.
- 679 Muhammad Maaz, Hanoona Rasheed, Salman Khan, and Fahad Khan. Videogpt+: Integrating
 680 image and video encoders for enhanced video understanding. *arXiv:2406.09418*, 2024.
- 682 Antoine Miech, Dimitri Zhukov, Jean-Baptiste Alayrac, Makarand Tapaswi, Ivan Laptev, and Josef
 683 Sivic. Howto100m: Learning a text-video embedding by watching hundred million narrated video
 684 clips. In *ICCV*, pp. 2630–2640, 2019.
- 686 WonJun Moon, Sangeek Hyun, SangUk Park, Dongchan Park, and Jae-Pil Heo. Query-dependent
 687 video representation for moment retrieval and highlight detection. In *CVPR*, pp. 23023–23033,
 688 2023.
- 689 OpenAI. Gpt-4v(ision) system card, 2023. URL <https://openai.com/index/gpt-4v-system-card/>.
- 692 OpenAI. Gpt-4o system card, 2024a. URL <https://openai.com/index/gpt-4o-system-card/>.
- 695 OpenAI. Openai o1 system card, 2024b. URL <https://openai.com/index/openai-o1-system-card/>.
- 697 OpenAI. Gpt-5 system card, 2025. URL <https://openai.com/index/gpt-5-system-card/>.
- 700 OpenGVLab. Internvl2: Better than the best—expanding performance boundaries of open-source
 701 multimodal models with the progressive scaling strategy, 2024. URL <https://internvl.github.io/blog/2024-07-02-InternVL-2.0/>.

- 702 Long Qian, Juncheng Li, Yu Wu, Yaobo Ye, Hao Fei, Tat-Seng Chua, Yueling Zhuang, and Siliang
 703 Tang. Momentor: Advancing video large language model with fine-grained temporal reasoning.
 704 *arXiv:2402.11435*, 2024a.
- 705 Rui Qian, Xiaoyi Dong, Pan Zhang, Yuhang Zang, Shuangrui Ding, Dahua Lin, and Jiaqi Wang.
 706 Streaming long video understanding with large language models. In *NeurIPS*, pp. 119336–
 707 119360, 2024b.
- 708 Mengxue Qu, Xiaodong Chen, Wu Liu, Alicia Li, and Yao Zhao. Chatvtg: Video temporal ground-
 709 ing via chat with video dialogue large language models. In *CVPR*, pp. 1847–1856, 2024.
- 710 Santhosh Kumar Ramakrishnan, Ziad Al-Halah, and Kristen Grauman. Naq: Leveraging narrations
 711 as queries to supervise episodic memory. In *CVPR*, pp. 6694–6703, 2023.
- 712 Michaela Regneri, Marcus Rohrbach, Dominikus Wetzel, Stefan Thater, Bernt Schiele, and Manfred
 713 Pinkal. Grounding action descriptions in videos. *Transactions of the Association for Compu-
 714 tational Linguistics*, 1:25–36, 2013.
- 715 Machel Reid, Nikolay Savinov, Denis Teplyashin, Dmitry Lepikhin, Timothy Lillicrap, Jean-
 716 baptiste Alayrac, Radu Soricut, Angeliki Lazaridou, Orhan Firat, Julian Schrittwieser, et al.
 717 Gemini 1.5: Unlocking multimodal understanding across millions of tokens of context.
 718 *arXiv:2403.05530*, 2024.
- 719 Shuhuai Ren, Linli Yao, Shicheng Li, Xu Sun, and Lu Hou. Timechat: A time-sensitive multimodal
 720 large language model for long video understanding. In *CVPR*, pp. 14313–14323, 2024.
- 721 Noah Shinn, Federico Cassano, Ashwin Gopinath, Karthik Narasimhan, and Shunyu Yao. Reflexion:
 722 Language agents with verbal reinforcement learning. In *NeurIPS*, pp. 8634–8652, 2023.
- 723 David Silver, Aja Huang, Chris J Maddison, Arthur Guez, Laurent Sifre, George Van Den Driessche,
 724 Julian Schrittwieser, Ioannis Antonoglou, Veda Panneershelvam, Marc Lanctot, et al. Mastering
 725 the game of go with deep neural networks and tree search. *Nature*, 529(7587):484–489, 2016.
- 726 Enxin Song, Wenhao Chai, Guanhong Wang, Yucheng Zhang, Haoyang Zhou, Feiyang Wu, Xun
 727 Guo, Tian Ye, Yan Lu, Jenq-Neng Hwang, et al. Moviechat: From dense token to sparse memory
 728 for long video understanding. *arXiv:2307.16449*, 2023.
- 729 Didac Suris, Sachit Menon, and Carl Vondrick. Vipergpt: Visual inference via python execution for
 730 reasoning. In *ICCV*, pp. 11888–11898, 2023.
- 731 Siyu Teng, Xuemin Hu, Peng Deng, Bai Li, Yuchen Li, Yunfeng Ai, Dongsheng Yang, Lingxi Li,
 732 Zhe Xuanyuan, Fenghua Zhu, et al. Motion planning for autonomous driving: The state of the art
 733 and future perspectives. *IEEE Transactions on Intelligent Vehicles*, 8(6):3692–3711, 2023.
- 734 Omkar Thawakar, Dinura Dissanayake, Ketan More, Ritesh Thawkar, Ahmed Heakl, Noor Ahsan,
 735 Yuhao Li, Mohammed Zumri, Jean Lahoud, Rao Muhammad Anwer, et al. Llamav-o1: Rethink-
 736 ing step-by-step visual reasoning in llms. *arXiv:2501.06186*, 2025.
- 737 Ashish Vaswani, Noam Shazeer, Niki Parmar, Jakob Uszkoreit, Llion Jones, Aidan N Gomez,
 738 Lukasz Kaiser, and Illia Polosukhin. Attention is all you need. In *NeurIPS*, pp. 5998–6008,
 739 2017.
- 740 Ante Wang, Linfeng Song, Ye Tian, Baolin Peng, Dian Yu, Haitao Mi, Jinsong Su, and Dong Yu.
 741 Litesearch: Efficacious tree search for llm. *arXiv:2407.00320*, 2024a.
- 742 Haibo Wang, Zhiyang Xu, Yu Cheng, Shizhe Diao, Yufan Zhou, Yixin Cao, Qifan Wang, Weifeng
 743 Ge, and Lifu Huang. Grounded-videollm: Sharpening fine-grained temporal grounding in video
 744 large language models. *arXiv:2410.03290*, 2024b.
- 745 Peng Wang, Shuai Bai, Sinan Tan, Shijie Wang, Zhihao Fan, Jinze Bai, Keqin Chen, Xuejing Liu,
 746 Jialin Wang, Wenbin Ge, et al. Qwen2-vl: Enhancing vision-language model’s perception of the
 747 world at any resolution. *arXiv:2409.12191*, 2024c.

- 756 Weihuan Wang, Zehai He, Wenyi Hong, Yean Cheng, Xiaohan Zhang, Ji Qi, Xiaotao Gu, Shiyu
 757 Huang, Bin Xu, Yuxiao Dong, et al. Lvbench: An extreme long video understanding benchmark.
 758 *arXiv:2406.08035*, 2024d.
- 759 Xiaohan Wang, Yuhui Zhang, Orr Zohar, and Serena Yeung-Levy. Videoagent: Long-form video
 760 understanding with large language model as agent. *arXiv:2403.10517*, 2024e.
- 762 Xiyao Wang, Ruijie Zheng, Yanchao Sun, Ruonan Jia, Wichayaporn Wongkamjan, Huazhe Xu,
 763 and Furong Huang. Coplanner: Plan to roll out conservatively but to explore optimistically for
 764 model-based rl. *arXiv:2310.07220*, 2023.
- 766 Xiyao Wang, Linfeng Song, Ye Tian, Dian Yu, Baolin Peng, Haitao Mi, Furong Huang, and Dong
 767 Yu. Towards self-improvement of llms via mcts: Leveraging stepwise knowledge with curriculum
 768 preference learning. *arXiv:2410.06508*, 2024f.
- 769 Yueqian Wang, Xiaojun Meng, Jianxin Liang, Yuxuan Wang, Qun Liu, and Dongyan Zhao. Hawk-
 770 eye: Training video-text llms for grounding text in videos. *arXiv:2403.10228*, 2024g.
- 772 Jason Wei, Xuezhi Wang, Dale Schuurmans, Maarten Bosma, Fei Xia, Ed Chi, Quoc V Le, Denny
 773 Zhou, et al. Chain-of-thought prompting elicits reasoning in large language models. In *NeurIPS*,
 774 pp. 24824–24837, 2022.
- 775 Haoning Wu, Dongxu Li, Bei Chen, and Junnan Li. Longvideobench: A benchmark for long-context
 776 interleaved video-language understanding. In *NeurIPS*, pp. 28828–28857, 2024.
- 778 Jianlong Wu, Wei Liu, Ye Liu, Meng Liu, Liqiang Nie, Zhouchen Lin, and Chang Wen Chen. A
 779 survey on video temporal grounding with multimodal large language model. *arXiv:2508.10922*,
 780 2025.
- 781 Junbin Xiao, Xindi Shang, Angela Yao, and Tat-Seng Chua. Next-qa: Next phase of question-
 782 answering to explaining temporal actions. In *CVPR*, pp. 9777–9786, 2021.
- 784 Junbin Xiao, Angela Yao, Yicong Li, and Tat-Seng Chua. Can i trust your answer? visually grounded
 785 video question answering. In *CVPR*, pp. 13204–13214, 2024.
- 786 Guowei Xu, Peng Jin, Li Hao, Yibing Song, Lichao Sun, and Li Yuan. Llava-cot: Let vision
 787 language models reason step-by-step. In *ICCV*, 2025.
- 789 Lin Xu, Yilin Zhao, Daquan Zhou, Zhijie Lin, See Kiong Ng, and Jiashi Feng. Pllava: Parameter-
 790 free llava extension from images to videos for video dense captioning. *arXiv:2404.16994*, 2024a.
- 792 Yuancheng Xu, Udari Madhushani Sehwag, Alec Koppel, Sicheng Zhu, Bang An, Furong Huang,
 793 and Sumitra Ganesh. Genarm: Reward guided generation with autoregressive reward model for
 794 test-time alignment. *arXiv:2410.08193*, 2024b.
- 795 Ziang Yan, Zhilin Li, Yinan He, Chenting Wang, Kunchang Li, Xinhao Li, Xiangyu Zeng, Zilei
 796 Wang, Yali Wang, Yu Qiao, et al. Task preference optimization: Improving multimodal large
 797 language models with vision task alignment. *arXiv:2412.19326*, 2024.
- 798 Antoine Yang, Antoine Miech, Josef Sivic, Ivan Laptev, and Cordelia Schmid. Zero-shot video
 799 question answering via frozen bidirectional language models. *Advances in Neural Information
 800 Processing Systems*, 35:124–141, 2022.
- 802 Zhengyuan Yang, Linjie Li, Jianfeng Wang, Kevin Lin, Ehsan Azarnasab, Faisal Ahmed, Zicheng
 803 Liu, Ce Liu, Michael Zeng, and Lijuan Wang. Mm-react: Prompting chatgpt for multimodal
 804 reasoning and action. *arXiv:2303.11381*, 2023.
- 805 Shunyu Yao, Dian Yu, Jeffrey Zhao, Izhak Shafran, Tom Griffiths, Yuan Cao, and Karthik
 806 Narasimhan. Tree of thoughts: Deliberate problem solving with large language models. In
 807 *NeurIPS*, pp. 11809–11822, 2023a.
- 809 Shunyu Yao, Jeffrey Zhao, Dian Yu, Nan Du, Izhak Shafran, Karthik Narasimhan, and Yuan Cao.
 810 React: Synergizing reasoning and acting in language models. In *ICLR*, 2023b.

- 810 Shoubin Yu, Jaemin Cho, Prateek Yadav, and Mohit Bansal. Self-chained image-language model
 811 for video localization and question answering. In *NeurIPS*, pp. 76749–76771, 2023.
- 812
- 813 Ce Zhang, Taixi Lu, Md Mohaiminul Islam, Ziyang Wang, Shoubin Yu, Mohit Bansal, and Gedas
 814 Bertasius. A simple Llm framework for long-range video question-answering. *arXiv:2312.17235*,
 815 2023a.
- 816 Chen-Lin Zhang, Jianxin Wu, and Yin Li. Actionformer: Localizing moments of actions with
 817 transformers. In *ECCV*, pp. 492–510, 2022.
- 818
- 819 Dan Zhang, Sining Zhoubian, Ziniu Hu, Yisong Yue, Yuxiao Dong, and Jie Tang. Rest-mcts*: Llm
 820 self-training via process reward guided tree search. *arXiv:2406.03816*, 2024a.
- 821 Hang Zhang, Xin Li, and Lidong Bing. Video-llama: An instruction-tuned audio-visual language
 822 model for video understanding. *arXiv:2306.02858*, 2023b.
- 823
- 824 Hao Zhang, Aixin Sun, Wei Jing, and Joey Tianyi Zhou. Span-based localizing network for natural
 825 language video localization. *arXiv:2004.13931*, 2020a.
- 826 Peiyuan Zhang, Kaichen Zhang, Bo Li, Guangtao Zeng, Jingkang Yang, Yuanhan Zhang, Ziyue
 827 Wang, Haoran Tan, Chunyuan Li, and Ziwei Liu. Long context transfer from language to vision.
 828 *arXiv:2406.16852*, 2024b.
- 829
- 830 Songyang Zhang, Houwen Peng, Jianlong Fu, and Jiebo Luo. Learning 2d temporal adjacent net-
 831 works for moment localization with natural language. In *AAAI*, pp. 12870–12877, 2020b.
- 832 Zhuosheng Zhang, Aston Zhang, Mu Li, Hai Zhao, George Karypis, and Alex Smola. Multimodal
 833 chain-of-thought reasoning in language models. *arXiv:2302.00923*, 2023c.
- 834
- 835 Yue Zhao, Ishan Misra, Philipp Krahenbuhl, and Rohit Girdhar. Learning video representations
 836 from large language models. In *CVPR*, pp. 6586–6597, 2023.
- 837 Junjie Zhou, Yan Shu, Bo Zhao, Boya Wu, Shitao Xiao, Xi Yang, Yongping Xiong, Bo Zhang,
 838 Tiejun Huang, and Zheng Liu. Mlvu: A comprehensive benchmark for multi-task long video
 839 understanding. *arXiv:2406.04264*, 2024.
- 840
- 841 Jinguo Zhu, Weiyun Wang, Zhe Chen, Zhaoyang Liu, Shenglong Ye, Lixin Gu, Yuchen Duan, Hao
 842 Tian, Weijie Su, Jie Shao, et al. Internvl3: Exploring advanced training and test-time recipes for
 843 open-source multimodal models. *arXiv:2504.10479*, 2025.
- 844
- 845
- 846
- 847
- 848
- 849
- 850
- 851
- 852
- 853
- 854
- 855
- 856
- 857
- 858
- 859
- 860
- 861
- 862
- 863

864 APPENDIX
865866 In this appendix, we provide more details about the model inference pipeline and implementation
867 details to complement the main paper. Additional experiments, [detailed analysis](#), and discussions
868 are also incorporated. Below is the table of contents.
869

- 870 **A. Model**
- 871 1. Inference Pipeline
- 872 2. Implementation Details
- 873 **B. Experiments**
- 874 1. Benchmarks and Settings
- 875 2. More Experimental Results
- 876 3. More [Detailed Analysis](#)
- 877 **C. Miscellaneous**
- 878 1. Prompt Templates
- 879 **D. The Use of LLMs Statement**
- 880

883 **A MODEL**885 **A.1 INFERENCE PIPELINE**887 The formulation of VideoMind’s inference pipeline is illustrated in Algorithm 1. Given a video \mathcal{V}
888 and a question \mathcal{Q} , the planner dynamically calls different roles on demand to analyze the multi-
889 modal context and generate the answer.891 **Algorithm 1** VideoMind’s Chain-of-LoRA Pipeline

```

1: Input: A video  $\mathcal{V}$  and a question  $\mathcal{Q}$ 
2: Output: An answer  $\mathcal{A}$  to the question with temporal moment  $\mathcal{T} = [t_s, t_e]$ 
3: Plan  $\mathcal{P} \leftarrow \text{Planner}(\mathcal{V}, \mathcal{Q})$ 
4: if Grounder  $\in \mathcal{P}$  then
5:     $\{[t_s^i, t_e^i]\}_i \leftarrow \text{Grounder}(\mathcal{V}, \mathcal{Q})$ 
6:    for all  $i$  do
7:      $\tilde{\mathcal{V}}_i \leftarrow \text{ZoomIn}(\mathcal{V}, [t_s^i, t_e^i])$ 
8:      $Score_i \leftarrow \text{Verifier}(\tilde{\mathcal{V}}_i, \mathcal{Q})$ 
9:    end for
10:     $i \leftarrow \arg \max s_i(Score_i)$ 
11: end if
12: if Answerer  $\in \mathcal{P}$  then
13:     $\mathcal{A} \leftarrow \text{Answerer}(\tilde{\mathcal{V}}_i, \mathcal{Q})$ 
14: end if
15: return  $(\mathcal{A}, \mathcal{T})$ 

```

906 **A.2 IMPLEMENTATION DETAILS**908 We leverage the 2B and 7B versions of Qwen2-VL (Wang et al., 2024c) as our base models, and
909 apply LoRA adapters with rank = 64 and alpha = 64 to the planner, grounder, and verifier. The
910 hidden size of the timestamp decoder is set to 256. The maximum number of tokens per frame
911 and maximum number of frames for the planner, grounder, verifier, and answerer are set as [64,
912 100], [64, 150], [64, 64], and [256, 32], respectively. We train different roles separately on different
913 datasets and load them together during inference, so that the model can efficiently switch roles by
914 activating different LoRAs. During training, we set the global batch size to 32, and utilize the
915 AdamW optimizer (Loshchilov & Hutter, 2019) with learning rates of 2e-5, 1e-4, and 5e-5 for
916 planner, grounder, and verifier, respectively. All the roles were trained for 1 epoch on their specific
917 datasets, with a linear warmup in the first 3% steps. During inference, we apply an NMS with
918 IoU = 0.75 to reduce duplicated moments from the grounder.

918
919 Table 9: Details of the evaluation benchmarks. The datasets encompass three representative tasks,
920 *i.e.*, Grounded VideoQA, Video Temporal Grounding, and General VideoQA, with video durations
921 ranging from several seconds to more than one hour.

Dataset	Duration	Domain	Main Metrics
<i>Grounded Video Question Answering (Grounding + QA)</i>			
CG-Bench (Chen et al., 2024a)	1624.4s	Diverse	rec. @IoU, acc. @IoU
ReXTime (Chen et al., 2024b)	141.1s	Vlog, News, Activity	mIoU, Acc (IoU ≥ 0.5)
NExT-GQA (Xiao et al., 2024)	39.5s	Reasoning	mIoP, Acc @GQA
<i>Video Temporal Grounding (Grounding only)</i>			
Charades-STA (Gao et al., 2017)	30.1s	Indoor	R@{0.3 ~ 0.7}, mIoU
ActivityNet-Captions (Krishna et al., 2017)	111.4s	Activity	R@{0.3 ~ 0.7}, mIoU
QVHighlights (Lei et al., 2021)	150s	Vlog, News	R@{0.5, 0.7}, mAP
TACoS (Regneri et al., 2013)	358.2s	Cooking	R@{0.3 ~ 0.7}, mIoU
Ego4D-NLQ (Grauman et al., 2022)	379.0s	Egocentric	R@{0.3 ~ 0.7}, mIoU
ActivityNet-RTL (Huang et al., 2024b)	111.4s	Reasoning	P@0.5, mIoU
<i>General Video Question Answering (QA only)</i>			
Video-MME (Fu et al., 2024a)	1017.9s	Diverse	Acc (w/o subs)
MLVU (Zhou et al., 2024)	930s	Diverse	Acc
LVBench (Wang et al., 2024d)	4101s	Diverse	Acc
MVBench (Li et al., 2024b)	15s	Diverse	Acc
LongVideoBench (Wu et al., 2024)	473s	Diverse	Acc

938 Table 10: Performance on MultiHop-EgoQA (Chen et al., 2025a). FT means fine-tuning on the
939 target dataset. Sent. Sim. denotes sentence similarity computed by all-MiniLM-L6-v2.

Method	Size	FT	Temporal Grounding		Question Answering	
			IoU@0.3	mIoU	Sent. Sim.	Score
Human	–	–	87.0	61.8	74.3	7.5
GPT-4o (OpenAI, 2024a)	–	✗	12.0	12.2	73.7	5.4
InternVL2 (OpenGVLab, 2024)	8B	✗	6.3	6.6	71.9	4.5
LLaVA-NeXT-Video (Liu et al., 2024a)	7B	✗	–	–	62.1	4.2
TimeChat (Ren et al., 2024)	7B	✗	3.0	3.6	58.9	3.3
VTimeLLM (Huang et al., 2024a)	7B	✗	8.8	9.2	70.5	4.3
GeLM (Chen et al., 2025a)	7B	✓	18.2	16.7	<u>75.0</u>	4.8
VideoMind (Ours)	2B	✗	<u>23.2</u>	<u>17.8</u>	58.8	3.5
VideoMind (Ours)	7B	✗	<u>25.1</u>	<u>19.0</u>	<u>77.3</u>	4.9

B EXPERIMENTS

B.1 BENCHMARKS AND SETTINGS

951 The experiments are extensively designed across 14 diverse benchmarks. The statistics are listed in
952 Table 9. The major benchmarks are introduced below.

953 **CG-Bench (Chen et al., 2024a)** is designed for long video grounded question answering, featuring
954 a diverse domain and various evaluation metrics. It includes 1.2K manually curated videos, ranging
955 from 10 to 80 minutes, with a total of 12K QA pairs. The dataset is categorized into perception,
956 reasoning, and hallucination question types, and introduces clue-based evaluation methods like white
957 box and black box assessments to ensure models provide answers based on accurate video reasoning.

958 **ReXTime (Chen et al., 2024b)** tests models on complex temporal reasoning, using an automated
959 pipeline for QA pair generation, significantly reducing manual effort. It includes 921 validation
960 and 2.1K test samples, each manually curated for accuracy, and highlights a 14.3% accuracy gap
961 between SoTA models and human performance. This benchmark is crucial for evaluating models
962 on cause-and-effect relationships across video segments.

963 **NExT-GQA (Xiao et al., 2024)** aims to challenge models to reason about causal and temporal
964 actions, supporting both multi-choice and open-ended tasks. This is an extension of NExT-QA
965 (Xiao et al., 2021) comprising 10.5K manually labeled video QA pairs with temporal segments.
966 The samples in this benchmark are from “causal” and “temporal” classes, while the “descriptive”
967 questions in NExT-QA are discarded.

972
 973 Table 11: Video temporal grounding on TACoS (Regneri et al., 2013). FT means fine-tuning on the
 974 target dataset. Note that our method was co-trained on this dataset.

Method	Size	FT	R@0.3	R@0.5	R@0.7	mIoU
<i>Non-LLM-based Specialists</i>						
2D-TAN (Zhang et al., 2020b)	–	✓	40.0	28.0	12.9	27.2
Moment-DETR (Lei et al., 2021)	–	✓	38.0	24.7	12.0	25.5
UniVTG (Lin et al., 2023b)	–	✓	51.4	35.0	17.4	33.6
R ² -Tuning (Liu et al., 2024d)	–	✓	49.7	38.7	25.1	35.9
<i>LLM-based Generalists</i>						
VideoMind (Ours)	2B	✗	38.6	26.9	15.5	27.4
VideoMind (Ours)	7B	✗	49.5	36.2	21.4	34.4

981
 982 Table 12: Performance of video temporal grounding on Ego4D-NLQ (Grauman et al., 2022). FT
 983 means fine-tuning on the target dataset. **VideoMind-Ego** is a variant of our method trained with extra
 984 67K egocentric grounding samples from NaQ (Ramakrishnan et al., 2023).

Method	Size	FT	R@0.3	R@0.5	R@0.7	mIoU
<i>Non-LLM-based Specialists</i>						
2D-TAN (Zhang et al., 2020b)	–	✓	4.3	1.8	0.6	3.4
VSLNet (Zhang et al., 2020a)	–	✓	4.5	2.4	1.0	3.5
Moment-DETR (Lei et al., 2021)	–	✓	4.3	1.8	0.7	3.5
UniVTG (Lin et al., 2023b)	–	✓	7.3	4.0	1.3	4.9
R ² -Tuning (Liu et al., 2024d)	–	✓	7.2	4.5	2.1	4.9
UniVTG (Lin et al., 2023b)	–	✗	6.5	3.5	1.2	4.6
<i>LLM-based Generalists</i>						
VideoMind (Ours)	2B	✗	5.9	2.9	1.2	4.7
VideoMind (Ours)	7B	✗	7.2	3.7	1.7	5.4
VideoMind-Ego (Ours)	2B	✗	7.2	3.9	1.8	5.3

1000 **Charades-STA** (Gao et al., 2017) contains 10K in-door videos, averaging 30.1 seconds each, with
 1001 16K temporal annotations spanning daily activity, alongside free-text descriptions. These rich annotations
 1002 make Charades-STA particularly suitable for evaluating temporal grounding models under
 1003 indoor environments.

1004 **ActivityNet-Captions** (Krishna et al., 2017) is a large-scale benchmark with 20K untrimmed
 1005 YouTube videos with a total of 849 hours, covering diverse activities from personal care to sports.
 1006 This dataset contains high-quality dense video captioning annotations (3.65 temporally localized
 1007 sentences per video), which we use as queries for video temporal grounding. Each query has an
 1008 average length of 13.5 words.

1010 B.2 MORE EXPERIMENTAL RESULTS

1012 **Multi-Hop Grounded Question Answering** To investigate the performance of our method on
 1013 novel tasks that require a hybrid or dynamically generated sequence of steps, we evaluate our method
 1014 on MultiHop-EgoQA (Chen et al., 2025a), a Grounded VideoQA dataset highlighting multi-hop
 1015 temporal reasoning. For each question, the model must ground and reason on multiple relevant
 1016 moments before answering, which is a paradigm that does not fit neatly into the pre-defined single-hop
 1017 grounding pipeline. The evaluation results are shown in Table 10. Thanks to VideoMind’s archi-
 1018 tectural design to produce multiple candidate moments in a single grounding step, it can effectively
 1019 capture the multi-hop evidence required by this benchmark. As a result, our method achieves strong
 1020 zero-shot performance, surpassing all open-source baselines and remaining competitive to closed-
 1021 source GPT-4o (OpenAI, 2024a) across both grounding metrics and QA metrics.

1022 **Video Temporal Grounding** We additionally compare VideoMind with representative methods on
 1023 the challenging TACoS (Regneri et al., 2013), Ego4D-NLQ (Grauman et al., 2022), and QVHigh-
 1024 lights (Lei et al., 2021) datasets in Table 11, Table 12, and Table 13, respectively. Our 2B model
 1025 performs better than the strong task-specific baseline UniVTG (Lin et al., 2023b) on TACoS but
 slightly worse than it on Ego4D-NLQ. **This is justifiable as neither the grounder nor the verifier was**

1026
1027
1028

Table 13: Fine-tuned video temporal grounding results on QVHighlights (Lei et al., 2021).

Method	Size	R1		mAP		
		@0.5	@0.7	@0.5	@0.75	Avg.
<i>Non-LLM-based Specialists</i>						
XML (Lei et al., 2020)	–	41.83	30.35	44.63	31.73	32.14
XML+ (Lei et al., 2021)	–	46.69	33.46	47.89	34.67	34.90
Moment-DETR (Lei et al., 2021)	–	59.78	40.33	60.51	35.36	36.14
UMT (Liu et al., 2022)	–	60.83	43.26	57.33	39.12	38.08
MomentDiff (Li et al., 2023b)	–	58.21	41.48	54.57	37.21	36.84
QD-DETR (Moon et al., 2023)	–	62.40	44.98	62.52	39.88	39.86
UniVTG (Lin et al., 2023b)	–	65.43	50.06	64.06	45.02	43.63
R ² -Tuning (Liu et al., 2024d)	–	68.03	49.35	69.04	47.56	46.17
<i>LLM-based Generalists</i>						
VideoMind (Ours)	2B	75.42	59.35	74.11	55.15	51.60
VideoMind (Ours)	7B	78.53	61.09	76.07	58.17	54.19

1041

Table 15: Performance of VideoQA on LongVideoBench (Wu et al., 2024) val split.

Method	Size	Acc	Acc @ Duration Groups			
			(8, 15]	(15, 60]	(180, 600]	(900, 3600]
GPT-4o (OpenAI, 2024a)	–	66.7	71.4	76.7	69.1	60.9
GPT-4 Turbo (Achiam et al., 2023)	–	59.0	65.2	68.2	62.4	50.5
Gemini-1.5-Pro (Reid et al., 2024)	–	64.0	67.4	75.1	65.3	58.6
Gemini-1.5-Flash (Reid et al., 2024)	–	61.6	68.3	76.2	62.6	54.0
Idefics2 (Laurendon et al., 2024)	8B	49.7	59.8	65.7	47.8	42.7
Phi-3-Vision (Abdin et al., 2024)	4B	49.6	59.3	61.6	46.8	44.7
Mantis-Idefics2 (Jiang et al., 2024)	8B	47.0	56.6	55.8	45.6	42.2
Mantis-BakLLaVA (Jiang et al., 2024)	7B	43.7	53.4	57.6	40.3	38.7
VideoMind (Ours)	2B	48.8	59.3	59.3	49.3	41.7
VideoMind (Ours)	7B	56.3	67.7	67.4	56.8	48.6

1054

Table 16: Performance comparison on general VideoQA on MVBench (Li et al., 2024b).

Model	Size	AS	AP	AA	FA	UA	OE	OI	OS	MD	AL	ST	AC	MC	MA	SC	FP	CO	EN	ER	CI	Avg.
GPT-4V (OpenAI, 2023)	–	55.5	63.5	72.0	46.5	73.5	18.5	59.0	29.5	12.0	40.5	83.5	39.0	12.0	22.5	45.0	47.5	52.0	31.0	59.0	11.0	43.5
Video-ChatGPT (Maaaz et al., 2023)	7B	23.5	26.0	62.0	22.5	26.5	54.0	28.0	40.0	23.0	20.0	31.0	30.5	25.5	39.5	48.5	29.0	33.0	29.5	26.0	35.5	32.7
Video-LLaMA (Zhang et al., 2023b)	7B	27.5	25.5	51.0	29.0	39.0	48.0	40.5	38.0	22.5	22.5	43.0	34.0	22.5	32.5	45.5	32.5	40.0	30.0	21.0	37.0	34.1
VideoChat (Li et al., 2023a)	7B	33.5	26.5	56.0	33.5	40.5	53.0	40.5	30.0	25.5	27.0	48.5	35.0	20.5	42.5	46.0	26.5	41.0	23.5	23.5	36.0	35.5
Video-LLaVA (Lin et al., 2023a)	7B	46.0	42.5	56.5	39.0	53.5	53.0	48.0	41.0	29.0	31.5	82.5	45.0	26.0	53.0	41.5	33.5	41.5	27.5	38.5	31.5	43.0
TimeChat (Ren et al., 2024)	7B	40.5	36.0	61.0	32.5	53.0	53.5	41.5	29.0	19.5	26.5	66.5	34.0	20.0	43.5	42.0	36.5	36.0	29.0	35.0	35.0	38.5
PLLaVA (Xu et al., 2024a)	7B	58.0	49.0	55.5	41.0	61.0	56.0	61.0	36.0	23.5	26.0	82.0	39.5	42.0	52.0	45.0	42.0	53.5	30.5	48.0	31.0	46.6
ShareGPT4Video (Chen et al., 2024c)	7B	49.5	39.5	79.5	40.0	54.5	82.5	54.5	32.5	50.5	41.5	84.5	35.5	62.5	75.0	51.0	25.5	46.5	28.5	39.0	51.5	51.2
ST-LLM (Liu et al., 2024c)	7B	66.0	53.5	84.0	44.0	58.5	80.5	73.5	38.5	42.5	31.0	86.5	36.5	56.5	78.5	43.0	44.5	46.5	34.5	41.5	58.5	54.9
VideoGPT+ (Maaaz et al., 2024)	3.8B	69.0	60.0	83.0	48.5	66.5	85.5	75.5	36.0	44.0	34.0	89.5	39.5	71.0	90.5	45.0	53.0	50.5	29.5	44.0	60.0	58.7
VideoChat2 (Li et al., 2024b)	7B	75.5	58.0	83.5	50.5	60.5	87.5	74.5	45.0	47.5	44.0	82.5	37.0	64.5	87.5	51.0	66.5	47.0	35.0	37.0	72.5	60.4
VideoMind (Ours)	2B	78.5	76.0	75.5	46.0	69.5	90.5	71.5	33.0	48.0	40.0	92.5	52.5	71.5	92.0	44.5	61.5	61.5	37.5	51.0	57.0	62.5
VideoMind (Ours)	7B	74.0	71.5	81.0	50.0	77.0	93.0	75.0	38.0	48.5	46.0	91.0	39.0	80.0	94.5	49.5	55.5	70.0	40.5	57.0	61.0	64.6

1066

trained on egocentric videos, while UniVTG was pretrained on 1.8M samples from Ego4D (Grauman et al., 2022). To align the setting, we trained an additional VideoMind-2B variant with extra 67K grounding samples from NaQ (Ramakrishnan et al., 2023). To our best knowledge, VideoMind is **the first LLM-based grounding model that supports multi-moment outputs**, thereby being able to be evaluated on QVHighlights. Compared with task-specific experts, our VideoMind-2B significantly outperforms all previous methods and sets a new state-of-the-art.

1073

Reasoning Temporal Localization We also evaluate the generalizability of grounder and verifier on the more challenging reasoning temporal localization (Huang et al., 2024b) task, which is similar to video temporal grounding, but the queries are not directly describing the moment. The models are required to infer the actual event using their world knowledge. The results in Table 14 show that VideoMind can successfully generalize its zero-shot grounding capability to complex scenarios.

1079

General Video Question Answering For the task of long VideoQA, we also provide evaluations on LongVideoBench (Wu et al., 2024) in Table 15, which further verifies the effectiveness of Video-

Table 14: Comparison of performance on reasoning temporal localization on ActivityNet-RTL (Huang et al., 2024b). Our zero-shot VideoMind-7B outperforms the strong fine-tuned baseline LITA-13B (Huang et al., 2024b) by a considerable margin.						
Method	Size	FT	P@0.5	mIoU		
LITA (Huang et al., 2024b)	7B	✓	21.2	24.1		
LITA (Huang et al., 2024b)	13B	✓	25.9	28.6		

1080

1081 Table 17: Comparison with representative video reasoning methods on video QA/grounding tasks.

1082

1083

1084

1085

1086

1087

1088

1089

1090

1091

1092

1093

1094

1095

1096

1097

1098

1099

1100

1101

Method	Size	CG-Bench	MLVU	LVBench	Charades-STA	ActivityNet-Captions	
		long-acc.	M-Avg	Overall	R@0.5	mIoU	R@0.5
<i>Pure Text-based Reasoning Models</i>							
LongVILA-R1 (Chen et al., 2025b)	7B	26.7	56.5	34.7	30.3	30.0	16.4
Video-R1 (Feng et al., 2025)	7B	34.4	63.1	38.4	35.3	34.9	22.6
<i>Vision-centric Reasoning Models</i>							
VideoMind (Ours)	7B	38.4	64.4	40.8	59.1	50.2	30.3
							33.3

1090 Table 18: Performance of different timestamp modeling designs on Charades-STA (Gao et al., 2017).

1091

1092

1093

1094

1095

1096

1097

1098 Table 18: Performance of different timestamp modeling designs on Charades-STA (Gao et al., 2017).

Method	R@0.3	R@0.5	R@0.7	mIoU
Text-only (Ren et al., 2024)	56.8	39.5	14.3	36.1
Special Tokens (Qian et al., 2024a)	56.4	39.2	14.5	35.7
Embedding Matching (Liu et al., 2024e)	59.6	43.5	17.0	38.2
Time Marker (Chen et al., 2024d)	60.5	43.9	17.2	38.6
Timestamp Decoder (Ours)	64.1	47.2	21.7	42.0

1099 Table 19: Case distribution on ReXTime (Chen et al., 2024b) and NExT-GQA (Xiao et al., 2024).
1100 *Correct, Planning, Grounding, Verification, and Answering* refers to correct prediction, planning
1101 error, grounding error, verification error, and answering error, respectively.

1102

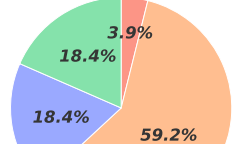
1103

1104

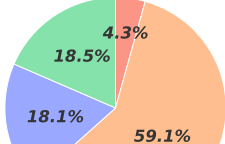
1105

1106

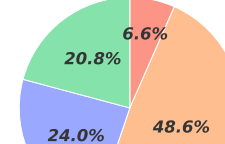
Method	Size	ReXTime				NExT-GQA			
		Correct	Planning	Grounding	Verification	Answering	Correct	Planning	Grounding
VideoMind	2B	69.1%	1.2%	18.3%	5.7%	5.7%	71.2%	1.9%	14.0%
VideoMind	7B	74.6%	1.1%	15.0%	4.6%	4.7%	76.6%	0.7%	11.8%



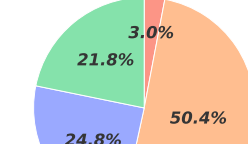
(a) ReXTime (2B)



(b) ReXTime (7B)



(c) NExT-GQA (2B)



(d) NExT-GQA (7B)

1117 Figure 7: Error distribution of our 2B and 7B variants on ReXTime (Chen et al., 2024b) and NExT-
1118 GQA (Xiao et al., 2024) datasets. The red, orange, blue, and green portions represent planning,
1119 grounding, verification, and answering errors, respectively.

1120

1121

1122

1123

1124 Mind on videos scaling to one-hour long. Table 16 presents more results of VideoMind on MVBench
1125 (Li et al., 2024b), which is a benchmark with very short videos (around 15s). Our model can still
1126 achieve good performance on these short video scenarios.

1127

1128

1129 **Comparison with Text-based Reasoning Models** In Table 17, we compare our method with
1130 representative pure text-based video reasoning methods. Our method significantly outperforms both
1131 baselines on all benchmarks, demonstrating that vision-centric reasoning is superior to pure text-
1132 based reasoning on long/complex video reasoning tasks.

1133

B.3 MORE DETAILED ANALYSIS

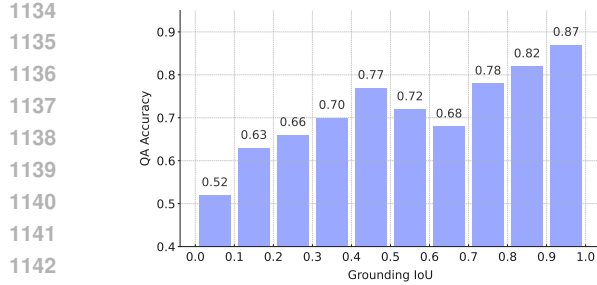
1134

1135

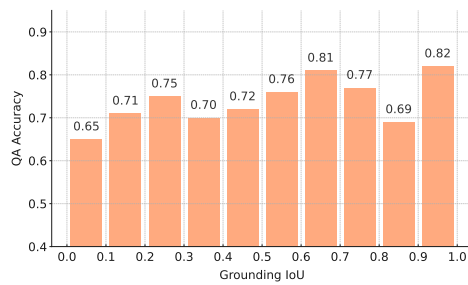
1136

1137

1138 **Timestamp Modeling Designs** The grounder plays a crucial role in our proposed Chain-of-LoRA
1139 pipeline. The model’s temporal grounding quality directly impacts the final QA accuracy. To demon-
1140 strate the necessity of this design, we implement and compare the following alternative timestamp
1141 modeling techniques based on VideoMind-2B (Grounder):



(a) ReXTime



(b) NExT-GQA

Figure 8: The correlation between grounding IoU and the final QA accuracy of VideoMind-2B on ReXTime (Chen et al., 2024b) and NExT-GQA (Xiao et al., 2024) datasets.

Table 20: Effect of the temporal feature pyramid on Charades-STA (Gao et al., 2017).

#Pyramid Levels	Charades-STA			
	R@0.3	R@0.5	R@0.7	mIoU
1	60.55	44.57	15.82	38.13
2	61.51	46.90	19.36	40.43
3	62.62	47.02	20.08	41.27
4	63.55	47.23	21.69	42.02

Table 21: Effect of different verifier styles on Charades-STA (Gao et al., 2017).

Verifier Type	Charades-STA			
	R@0.3	R@0.5	R@0.7	mIoU
Direct	60.42	45.28	19.32	39.84
Expand	65.10	48.70	23.15	43.57
Textual	65.24	49.33	23.89	44.01
Special Token	67.63	51.05	25.99	45.22

Table 22: Effect of the verifier on Charades-STA (Gao et al., 2017). IoU Raise means the percentage of the samples whose grounding IoU is raised by the verifier.

Role(s)	Size	R@0.3	R@0.5	R@0.7	mIoU	IoU Raise
Grounder	2B	63.2	46.9	20.5	41.7	–
Grounder + Verifier	2B	68.0 (+7.6%)	51.2 (+9.2%)	24.3 (+18.5%)	44.8 (+7.4%)	32.9%
Grounder	7B	69.4	53.2	26.6	46.8	–
Grounder + Verifier	7B	73.8 (+6.3%)	59.1 (+11.1%)	30.1 (+13.2%)	49.8 (+6.4%)	31.3%

Table 23: The accuracy of planner with different input combinations.

Input Video	Input Question	Planning Acc
✓	✓	0.42
✓	✓	0.79
✓	✓	0.93

Table 24: Comparison of average inference time on CG-Bench (Chen et al., 2024a) (avg. duration: 27 min).

Method	Size	Inference Time (s/video)
LongVILA-R1 (Chen et al., 2025b)	7B	<u>8.75</u>
VideoMind	7B	9.53 (+8.9%)
VideoMind (w. Auto Planning)	7B	8.07 (-7.8%)

1. **Text-only** (Ren et al., 2024): Directly represent timestamps in text form (e.g., “2.3 seconds”).
2. **Special Tokens** (Qian et al., 2024a): Define a set of timestamp tokens (e.g., <T0>, <T1>).
3. **Embedding Matching** (Liu et al., 2024e): Predict frame features to retrieve the frame index.
4. **Time Marker** (Chen et al., 2024d): Explicitly insert textual timestamps among visual tokens.

Their zero-shot video temporal grounding results are shown in Table 18. The results clearly demonstrate that the timestamp decoder delivers the strongest temporal grounding capability. We attribute it to two key factors: (1) It decouples continuous timestamp modeling from discrete token prediction, allowing the model to represent time with higher precision; (2) The direct regression supervision (L1 Loss) further enhances time reasoning and stabilizes training. Moreover, the timestamp decoder naturally supports predicting multiple moments with corresponding confidence scores, supporting tasks like multi-moments retrieval (Lei et al., 2021) and facilitating moment re-ranking through the verifier. These advantages jointly enhance the reliability of temporal grounding, which ensures the correct moment could be localized for further reasoning.

Effect of the Temporal Feature Pyramid Table 20 studies the effectiveness of the temporal feature pyramid. Our baseline model directly makes predictions on the last-layer transformer outputs. When adding more pyramid levels, the performance of video temporal grounding consistently im-

1188
1189
1190

Table 25: Controlled experiments with strictly aligned hyperparameter settings. Both MLVU (Zhou et al., 2024) and LVBench (Wang et al., 2024d) are downsampled to 300 samples each.

Method	Size	MLVU (mini)		LVBench (mini)	
		M-Avg	Overall	M-Avg	Overall
GPT-4o (OpenAI, 2024a)	–	59.7	31.3		
Gemini-1.5-Pro (Reid et al., 2024)	–	60.3	36.3		
VideoMind (Ours)	2B	59.3	35.7		
VideoMind (Ours)	7B	62.7	40.3		

1191
1192
1193
1194
1195
1196
1197

Table 26: Performance comparison among the integration of our Chain-of-LoRA mechanism on different representative base models.

Base Model	Size	CG-Bench		ReXTime		Video-MME		MLVU		LVBench	
		acc.@IoU	Acc@IoU	w/o sub.	M-Avg	Overall	M-Avg	Overall	M-Avg	Overall	
Qwen2-VL (Wang et al., 2024c)	2B	4.0	17.3	55.4	58.7	35.4					
	7B	4.7	20.2	58.2	64.4	40.8					
Qwen2.5-VL (Bai et al., 2025)	3B	5.0	15.6	60.9	62.7	40.5					
	7B	5.7	19.8	65.9	66.3	45.2					
InternVL3 (Zhu et al., 2025)	2B	4.1	17.5	58.2	61.4	38.1					
	8B	4.5	20.8	66.5	63.8	42.3					

1200
1201
1202
1203
1204
1205
1206
1207
1208

Table 27: Performance of the simulated multi-role pipelines on closed-source models. Both MLVU (Zhou et al., 2024) and LVBench (Wang et al., 2024d) are downsampled to 300 samples each.

Method	Multi-Role Pipeline	MLVU (mini)		LVBench (mini)	
		M-Avg	Overall	M-Avg	Overall
GPT-4o (OpenAI, 2024a)	✗	59.7	31.3		
	✓	62.3 (+4.4%)	32.7 (+4.5%)		
GPT-5 (OpenAI, 2025)	✗	61.7	34.3		
	✓	63.3 (+2.6%)	36.3 (+5.8%)		
Gemini-2.5-Pro (DeepMind, 2025)	✗	73.3	65.7		
	✓	76.3 (+4.1%)	68.7 (+4.6%)		

1209

1210
1211
1212
1213
1214
1215
1216
1217
1218
1219
1220
1221
1222
1223
1224
1225
1226
1227
1228
1229
1230
1231
1232
1233
1234
1235
1236
1237
1238
1239
1240
1241

proves under all metrics on Charades-STA (Gao et al., 2017) under zero-shot setting, suggesting the effectiveness of improving the robustness of the model when facing moments with different lengths.

Effect of the Verifier for Zoom-in Evaluation To quantify the verifier’s corrective gain, we provide a comparison between w. and w/o the verifier on Charades-STA (Gao et al., 2017) in Table 22. The results demonstrate that the verifier consistently enhances temporal grounding performance, especially on high-quality predictions (e.g., 18.5% higher R@0.7 on the 2B variant), highlighting its importance in the overall pipeline.

Design Choices of Verifier In Table 21, we examine various design choices for the verifier. The term “Direct” refers to the method where the grounded moment is directly sent into the model without any expansion. “Expand” denotes expanding the temporal boundaries by 50%, while “Textual” involves adding supplementary textual information to indicate the length of the target event. “Special Token” represents our final approach, utilizing special tokens to denote the grounded start and end timestamps. The comparison demonstrates that expanding the temporal boundaries effectively broadens the verifier’s perceptual range, and the use of special tokens enhances the model’s awareness of precise moment boundaries.

Reliability of the Planner We provide an in-depth investigation into the reliability of the planner. Specifically, we randomly split the planner’s training dataset into an 80% training set and a 20% test set, and then re-train the planner on the training set and evaluate it as a three-way classification task on the held-out test set. The metric planning accuracy is defined as the proportion of samples for which the predicted reasoning plan is correct. The comparison among different input combinations in Table 23 demonstrate that incorporating both video (even with low resolution) and question input substantially improves planning performance, and the resulting 93% accuracy reflects the considerable reliability of the planner.

1242 **Inference-Time Efficiency** In Table 24, we study the inference-time efficiency of our method on
 1243 CG-Bench (Chen et al., 2024a). All experiments are conducted on a single NVIDIA RTX 6000 Ada
 1244 GPU. Compared with the text-based reasoning baseline LongVILA-R1 (Chen et al., 2025b), our full
 1245 pipeline is approximately 8.9% slower. However, this gap can be easily bridged by activating the
 1246 planner’s auto-planning capability. When the planner is allowed to choose the reasoning path, some
 1247 easy questions are routed directly to the answerer, which substantially reduces the average inference
 1248 time from 9.53s to 8.07s per video, resulting 7.8% faster inference speed than the baseline.

1249 **Overall Robustness and Error Accumulation** We acknowledge that the proposed sequential
 1250 reasoning pipeline has the potential risk of error propagation and accumulation. To quantify this effect,
 1251 we conduct a systematic analysis of error propagation on two representative datasets: ReXTime
 1252 (Chen et al., 2024b) (more temporal-related) and NExT-GQA (Xiao et al., 2024) (more reasoning-
 1253 related). For both datasets, each error case is categorized into one of the following types: (1) **Plan-
 1254 ning Error**: The question can only be correctly answered by switching to another reasoning plan
 1255 (*e.g.*, from “all roles” to “answerer only”); (2) **Grounding Error**: All the top-5 predicted moments
 1256 are incorrect (*i.e.*, having temporal IoU < 0.5); (3) **Verification Error**: The moment selected after
 1257 verification is incorrect; (4) **Answering Error**: The predicted answer is incorrect.

1258 We present the case distributions in Table 19 and error distributions in Figure 7. Several conclusions
 1259 can be drawn from the results: (1) The planner is highly reliable, accounting for less than 5% of the
 1260 error cases on both datasets; (2) Grounding errors account for roughly half of all failures. This is
 1261 aligned with our hypothesis that accurate temporal grounding plays a crucial role in the multi-role
 1262 reasoning pipeline; (3) Verification and answering contribute comparably smaller portions of the
 1263 failures, accounting for only about 20% error cases each.

1264 **Correlation between Grounding IoU and QA Accuracy** We study the correlation between temporal
 1265 grounding performance and QA accuracy in Figure 8. Specifically, we group the samples in
 1266 ReXTime (Chen et al., 2024b) and NExT-GQA (Xiao et al., 2024) datasets into different IoU buckets,
 1267 and plot the average QA accuracy within each bucket. On ReXTime, which is more temporal-
 1268 related, the results show a clear positive correlation between grounding IoU and final QA accuracy.
 1269 On the more reasoning-related NExT-GQA, such correlation is less significant.

1270 **Controlled Experiments on Closed-source APIs** The results of closed-source models in Table 2
 1271 and Table 6 are reported from the corresponding benchmark papers, without strictly aligned settings.
 1272 Therefore, we provide a controlled experiment to validate the advantages of our method. Specific-
 1273 ally, we select two challenging long video understanding benchmarks, *i.e.*, MLVU (Zhou et al.,
 1274 2024) and LVbench (Wang et al., 2024d), and randomly sample 300 QA pairs from each, forming
 1275 MLVU (mini) and LVbench (mini). We align the key hyperparameters as follows:

1. **Frame Rate:** 1 FPS
2. **Max Frame Count:** 150
3. **Frame Resolution:** max 448×448 pixels with natural aspect ratio
4. **Model Hyperparameters:** $\text{temperature} = 0, \text{top_p} = 0, \text{top_k} = 0$

1276 The comparisons are presented in Table 25, clearly showing that our VideoMind-7B outperforms
 1277 both GPT-4o (OpenAI, 2024a) and Gemini-1.5-Pro (Reid et al., 2024) on both datasets.

1278 **Integration with More Open-source LMMs** In Table 26, we study whether the proposed Chain-
 1279 of-LoRA pipeline provides a consistent benefit across different base models. The results show that
 1280 when integrated with stronger base models like Qwen2.5-VL (Bai et al., 2025) and InternVL3 (Zhu
 1281 et al., 2025), the performance of our Chain-of-LoRA pipeline could be further enhanced on multiple
 1282 long video benchmarks, highlighting our method’s generalizability.

1283 **Integration with Closed-source LMMs** We are also interested in whether the proposed multi-
 1284 role pipeline could be simulated via a series of prompts on closed-source models. To investigate
 1285 this, we evaluate the effectiveness of the multi-role reasoning prompt when applied to three models,
 1286 *i.e.*, GPT-4o (OpenAI, 2024a), GPT-5 (OpenAI, 2025), and Gemini-2.5-Pro (DeepMind, 2025), on
 1287 the previously constructed MLVU (mini) and LVbench (mini). The results in Table 27 show that
 1288 our pipeline consistently boosts the performance of different closed-source models, highlighting an
 1289 interesting finding: the multi-role reasoning pipeline itself can systematically enhance long video
 1290 reasoning, even without role-specific model designs or training.

1291
 1292
 1293
 1294
 1295

1296 **C MISCELLANEOUS**
12971298 **C.1 PROMPT TEMPLATES**
12991300 We present the prompts used in this work, including the input prompts for each role of VideoMind
1301 and the prompt for GPT-4o mini (OpenAI, 2024a) for data annotation.
13021303 **Prompt for the Planner:**
13041305 You are acting as the planner now. Given a question about the video, your task is to analyze the question
1306 and identify the best way to answer this question. You have access to the following tools:
13071308 Grounder: Accepts a text query and localizes the relevant video segment according to the query.
1309 Verifier: A tool supporting grounder by verifying the reliability of its outputs.
1310 Answerer: Answer a given question directly based on the whole video or a cropped video segment.
13111312 Your response must be a list in JSON format. A valid plan for reasoning could be “grounder, ver-
1313 ifier, answer”, “grounder, verifier”, or “answerer”, depending on the given question. Please see an
1314 example of the format below.
13151316

```
[{"type": "grounder", "value": "text query"}, {"type": "verifier"}, {"type": "answerer"}]
```

1317 Note that only the grounder can accept an argument called “value”, which is the text query used
1318 for grounding. Now I give you the question: “{question}”. Please think carefully and respond with your
1319 plan in JSON directly.
13201321 **Prompt for the Grounder:**
13221323 You are acting as the grounder now. Given a video and a text query, your goal is to temporally localize
1324 the video moment described by the query. If the query is directly describing a moment, simply localize it
1325 according to its content. Otherwise, if the moment is described as “before/after a pivotal event”, you need
1326 to determine the actual event it refers to. The localized moment should only cover the target event. Now I
1327 give you the query: “{query}”. Please think carefully and provide your response.
13281329 **Prompt for the Verifier:**
13301331 You are acting as the verifier now. You will be presented a text query describing a moment that potentially
1332 happens in the given video. Your task is to identify whether the video segment between <SEG-START>
1333 and <SEG-END> perfectly covers the moment. If the described moment can be seen in the video, please
1334 focus on verifying whether the moment starts at <SEG-START> and ends at <SEG-END>. Respond with
1335 “Yes” if you think the moment boundaries are correct, otherwise “No”. If the described moment cannot
1336 be seen in the video, respond with “No” directly. Now I give you the query: “{query}”. Please think
1337 carefully and respond with “Yes” or “No” directly.
13381339 **Prompt for the Answerer:** When subtitles are considered, we only present the first 100 lines.
13401341 You are given a video with {duration} seconds long.
1342 Subtitles: {subtitles}
1343 {question}
1344 Options:
1345 (A) {option 1}
1346 (B) {option 2}
1347 (C) {option 3}
1348 (D) {option 4}
1349 Please only give the best option.1349 **Prompt for Query Rephrasing Data Generation:**

1350

1351 You are an expert in rewriting questions into queries. I will give you a question that requires to be
 1352 answered based on a specific moment in a video. Your task is to analyze the question and rewrite it into
 1353 a declarative sentence, which could be used as a text query to search for the relevant video moment. The
 1354 query should be concise, describing the key event or key scene that the question asks for.

1355

1356 Here are some examples:

1357

1358 Question: How does the male cyclist react when he sees the steep path?

1359 Query: The male cyclist sees the steep path.

1360

1361 Question: What did the girl do at the end of the video?

1362 Query: The end of the video.

1363

1364 Question: What did the lady do as she was cycling off?

1365 Query: The lady is cycling off.

1366

1367 Question: What is the person with red shirt doing on the yacht?

1368 Query: The person with red shirt stays on the yacht.

1369

1370 Now I give you the question: “{**question**}”. Please think carefully and respond with the query directly.

D THE USE OF LLMS STATEMENT

1371 Large Language Models (LLMs) were used in this study to aid in polishing the manuscript. Specif-
 1372 ically, we used LLMs to assist in refining the language and detecting potential grammatical errors.
 1373 This is to improve readability and ensure clarity of the paper. We confirm that LLMs were not in-
 1374 volved in research ideation, method exploration, and experiment designs. All research ideas, meth-
 1375 ods, and analysis were produced by the authors. We take full responsibility for the content in this
 1376 paper, including the text generated or polished by the LLMs.

1377

1378

1379

1380

1381

1382

1383

1384

1385

1386

1387

1388

1389

1390

1391

1392

1393

1394

1395

1396

1397

1398

1399

1400

1401

1402

1403